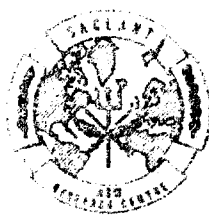


12

SACLANTGEN Report SR - 91

SACLANT ASW
RESEARCH CENTRE
REPORT



AD-A170 252

SYNTHETIC-APERTURE SONAR:
PERFORMANCE ANALYSIS OF BEAMFORMING
AND SYSTEM DESIGN

by
Ezio G. PUSONE
Lewis J. LLOYD

THIS FILE COPY

DTIC
ELECTE
JUL 28 1985
B

NOVEMBER 1985

**BEST
AVAILABLE COPY**

NORTH
ATLANTIC
TREATY
ORGANIZATION

SACLANTGEN
LA SPEZIA, ITALY

This document is unclassified. The information it contains is published subject to the conditions of the legend printed on the inside cover. Short quotations from it may be made in other publications if credit is given to the author(s). Except for working copies for research purposes, or for use in official NATO publications, reproduction requires the authorization of the Director of SACLANTGEN.

UNCLASSIFIED
EXEMPT FROM PUBLIC RELEASE
DATE 06-11-2001

SACLANICEN REPORT SR-91

NORTH ATLANTIC TREATY ORGANIZATION

SACLANT ASW Research Centre
Viale San Bartolomeo 400,
I-19026 San Bartolomeo (SP), Italy.

tel: national 0187 540111
international + 39 187 540111
telex: 271148 SACENT I

SYNTHETIC-APERTURE SONAR:
PERFORMANCE ANALYSIS OF
BEAMFORMING AND SYSTEM DESIGN

by

Ezio G. Pusone
Lewis J. Lloyd

November 1985

This report has been prepared as part of Project 02.

APPROVED FOR DISTRIBUTION

Ralph R. Goodman
RALPH R. GOODMAN
Director

DTIC
ELECTE
JUL 23 1986

B

DISTRIBUTION STATEMENT A
Approved for public release
Distribution Unlimited

TABLE OF CONTENTS

	<u>Pages</u>
ABSTRACT	1
INTRODUCTION	3
1 PASSIVE SYNTHETIC-APERTURE PROCESSING	5
1.1 Idealized Beamforming	5
1.2 Effect of Signal Coherence	6
1.3 Effect of Random Amplitude and Phase Fluctuations	6
1.4 Effect of Placement Errors	7
1.5 Results	8
2 ACTIVE SYNTHETIC-APERTURE PROCESSING	13
2.1 Active Idealized Beamforming	13
2.2 Effect of Random Amplitude & Phase Errors	16
2.3 Effect of Placement Errors	17
2.4 Simulation Results	18
CONCLUSIONS	21
REFERENCES	23
APPENDIX A - MATHEMATICAL DESCRIPTION OF THE PASSIVE SYNTHETIC-APERTURE BEAMFORMING PROCESS	25
APPENDIX B - MATHEMATICAL DESCRIPTION OF THE ACTIVE BEAMFORMING PROCESS	37

List of Figures

1. SAS - Passive mode	5
2. Passive SAS - Reasons for loss in performance	7
3. Effect of signal coherence time	10
4. Effect of random phase and amplitude errors	10
5. Effect of deterministic placement errors	10
6. Effect of random placement errors	11
7. Effect of 'weighting' in the presence of deterministic placement errors	11
8. SAS - Active mode	15
9. Reduction of undersampling sidelobes by using the beam pattern of the physical array	15
10. Geometry of the oscillating course	19
11. Active SAS - Synthesized beampattern	19

TABLE OF CONTENTS (Cont'd)List of Figures (Cont'd)

	<u>Pages</u>
12. Active SAS - Synthesized beam pattern	19
13. Active SAS - Effect of deterministic placement errors	20
14. Active SAS - Effect of deterministic placement errors	20
15. Active SAS - Effect of weighting in presence of deterministic placement errors	20
16. Active SAS - Effect of weighting in presence of deterministic placement errors	20
A1. Geometry for passive synthetic aperture mode	26
B1. Geometry of active ideal beamforming	38
B2. Timing sequence of active ideal beamforming	38
B3. Geometry of placement errors	49

SYNTHETIC-APERTURE SONAR: PERFORMANCE ANALYSIS OF
BEAMFORMING AND SYSTEM DESIGN

by

Ezio G. Pusone and Lewis J. Lloyd

ABSTRACT

Studies undertaken to assess the feasibility of applying synthetic-aperture techniques to sonar have been based on the theories developed for radar systems. They have been limited primarily to short-range, high-frequency active systems because the ratio of propagation speed to platform speed is much smaller than that encountered with radar. This study places emphasis on the beamforming aspects, the most important part of a synthetic-aperture system. A general approach is followed to develop a computer model to give estimates of beam patterns with active and passive modes of operation for a stationary target. The model allows the investigations of a number of features of the performance, for example the effect of random phase and amplitude fluctuations, of signal coherence time in the passive mode, and of both deterministic and random positional errors of the synthesizing array. In addition, the usefulness of weighting factors to steer and shape the synthesized beam is considered. The results presented give theoretical guidelines for the design of active and passive synthetic-aperture sonar systems.

✓
PER LETTER
ON FILE
DATE
A-1

INTRODUCTION

The aim of the synthetic-aperture technique is to obtain a high angular resolution from a small moving physical array by combining coherently the data from successive positions of the small array. It has been used successfully in aircraft and satellite active radar systems for which the speed of signal propagation is very much higher than the platform speed [1, 2].

In applications to sonar, the ratio of propagation and platform speeds is very much lower; consequently there are sampling problems. To date the applications in sonar have concentrated on uses for sea-bottom mapping [3, 4, 5] and mine-hunting systems [6].

Previous studies on applications to sonar [7, 8, 9, 10, 11, 12] have tended to take directly the results developed for radar, and have concentrated on short-range, high-frequency active systems. The present study builds up, for longer ranges and low-frequency systems, the beamforming process from a straightforward consideration of the phase of the received signals at successive positions of the physical array. This very basic approach is used to develop a computer model on SACLANTCEN's UNIVAC 1100/60 that allows various aspects of synthetic-aperture beamforming process to be investigated for a narrow-band passive system and for a multi-ping active sonar. The target/source is assumed to be stationary in both cases.

The computer model allows the investigations of the effects of the following features:

- a. Beam pattern of the physical array.
- b. Complex weighting functions for shaping and steering the synthesized beam.
- c. Lack of coherence in the received signals (passive mode only).
- d. Random perturbations in the amplitude and phase of the received signals.
- e. Placement errors due to a non-linear course of the physical array and to random positional errors.

The lack of coherence in the passive mode of operation referred to in (c) relates to a temporal (and possibly spatial) loss of coherence as the synthesizing array progresses along its synthesizing sequence. This is an area for which no published data in the open literature are available. Consequently a fairly simple assumption has been used in this report, namely that the coherence falls off exponentially with time.

The amplitude and phase fluctuations referred to in (d) could be caused by a number of factors, such as changes in the reflecting characteristics of the target as the synthesizing sequence progresses, fluctuations in the propagation path, or the presence of noise. In order to quantify these effects they have been related to the signal-to-noise power ratio at the output of the synthesizing array.

PRECEDING PAGE BLANK-NOT FILMED

Two types of placement errors (errors between the actual and assumed positions of the moving synthesizing array) have been investigated. One is a purely random positional error caused by, say, random navigation errors, and the other is a deterministic error caused by the array following a non-linear course that oscillates about the assumed straight-line track. This is the type of situation that can easily occur at sea when a ship attempts to follow a straight-line course but invariably "oscillates" around it.

We start with an analysis of the passive mode of operation because it is simpler to understand; we then consider the active mode.

1 PASSIVE SYNTHETIC-APERTURE PROCESSING

In the passive mode of operation, samples of the signal received at successive positions of the array as it moves through its synthesizing sequence are phase-compensated for the delay time and the movement of the array between samples, and then added coherently. The achieved performance obviously depends on the phase stability of each signal sample used in the coherent addition. We consequently attempt to analyze and assess the various possible sources of phase (and amplitude) errors.

The main assumptions for the passive mode of operation are that the radiating source a) is stationary, b) exhibits perfect spatial and temporal coherence that exists during the synthesizing period, and c) carries out own-doppler nullification before the synthetic beamforming process. With regard to the complex weighting factors (delay and steering vectors) used for beamforming, these are computed on the basis that the synthesizing array moves along an idealized straight-line course at a constant speed (U) and that the received signals are sampled at a constant sampling interval (Δt).

On the basis of these assumptions, a computer model has been developed using the equations derived in App. A. This model allows the computation of the synthesized beam pattern for the situations given below. The authors used the procedure described in [13].

1.1 Idealized Beamforming

The first situation assumed completely idealized parameters, full signal coherence for the total synthesizing period, no phase or amplitude errors, and no placement errors (Fig. 1). The general equation for the beampower output is Eq. A.8 of App. A:

$$P = \left[\sum_{k=1}^N A_k B_k \cos(\theta_{Sk} - \theta_{Fk}) \right]^2 + \left[\sum_{k=1}^N A_k B_k \sin(\theta_{Sk} - \theta_{Fk}) \right]^2 \quad (\text{Eq. 1})$$

In the far-field of the synthesized aperture this equation becomes the standard beam pattern expression for a linear array (see Eq. A.14 of App. A).

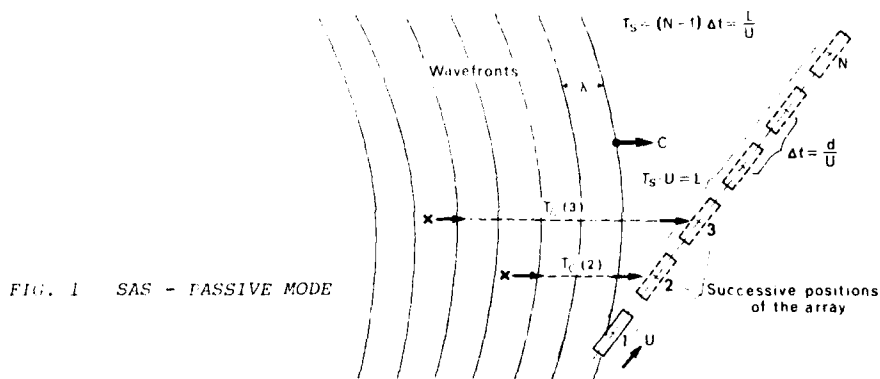


FIG. 1 SAS - PASSIVE MODE

1.2 Effect of Signal Coherence

The second situation assumed simply and plausibly that the signal coherence falls off exponentially with time. The expression for the synthesized beam pattern is now given by Eq. A.18 of App. A:

$$P = \sum_{k=1}^N S_k^2 + 2 \sum_{i=1}^{N-1} \sum_{k=1}^{N-i} \overline{S_k S_{k+i}} \exp(-|t_{k+i} - t_k|/T_c) \quad (\text{Eq. 2})$$

In this equation the parameter T_c is referred to as the "coherence time" of the signal.

1.3 Effect of Random Amplitude and Phase Fluctuations

Random amplitude and phase fluctuations could be caused by, for example, changes in the reflecting characteristics of the target/scatterer, by propagation effects, varying multipath structures, or the presence of noise. Characterizing these fluctuations is not easy, particularly because there exist no published data on fluctuations for a moving platform. Consequently we assume here that the fluctuations are a first-order Markov process. In order to quantify the fluctuations, we further assume that they have a root mean square (rms) value inversely proportional to the signal-to-noise power ratio at the "hydrophone" level, a mean value of zero, and a correlation time that varies exponentially from sample to sample (that is, with time). Thus, for example, the phase fluctuations are characterized by:

$$\overline{\varepsilon_k} = 0 \quad (\text{Eq. 3})$$

$$\overline{\varepsilon_k^2} = (S/N)^{-1} \quad (\text{Eq. 4})$$

$$E\{\varepsilon_k \cdot \varepsilon_{k+i}\} = \overline{\varepsilon_k \cdot \varepsilon_{k+i}} \exp(-|t_{k+i} - t_k|/T_E) \quad (\text{Eq. 5})$$

where T_E = correlation time, which is preselected.

When T_E is small, that is, when the correlation between errors is small, their effect is small. Alternatively, when T_E is large their effect is greater.

The resulting analytical equation for the effect of random amplitude (η) and of phase errors (ε) on the beam pattern is given by Eq. A.34 of App. A:

$$P = \sum_{k=1}^N A_k^2 f^2(\alpha_k) f^2(R_k) (b^2 + \overline{\eta^2}) + 2 \sum_{i=1}^{N-1} \sum_{k=1}^{N-i} [A_k f(\alpha_k) f(R_k) \cdot A_{k+i} f(\alpha_{k+i}) \cdot \{b^2 + \overline{\eta^2} \exp(-|t_{k+i} - t_k|/T_E)\} \cdot \{1 - \overline{\varepsilon_k^2} + \overline{\varepsilon_k^2} \exp(-|t_{k+i} - t_k|/T_E)\} \cdot \cos(\theta_k + \theta_{k+i})] \quad (\text{Eq. 6})$$

1.4 Effect of Placement Errors

By placement errors we mean the difference between the assumed and actual position of the synthesizing sequence; two types are investigated (see Fig. 2). First, the effect of the placement error due to random positional errors of the synthesizing array, (those for example caused by random navigational errors) is investigated. Second, the effect of the deterministic placement error due to the synthesizing array following a non-linear course that oscillates around an assumed straight-line course is examined. Because these errors are in terms of quantities that are not dimensionless their effect will be lessened by reducing the frequency of operation.

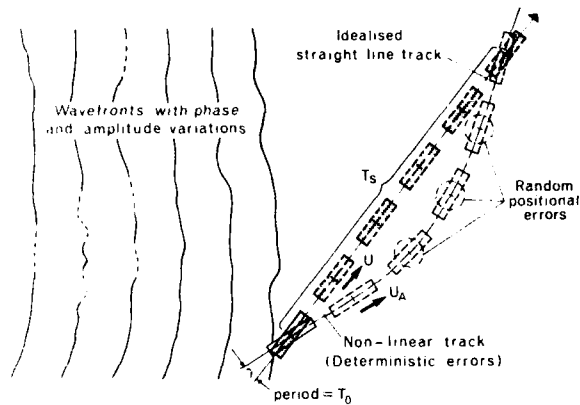


FIG. 2. PASSIVE SAS - REASONS FOR LOSS IN PERFORMANCE

1.4.1 Random Placement Errors

The random placement error is defined as a circular gaussian distribution of array positions about the assumed position. The errors are independent of each other and of the actual signal values. Thus the effect of these signals is independent of signal direction and can be characterized by a single standard deviation $\sigma(y)$. This can be converted into an effective variance of phase as follows:

$$\text{VAR}(\text{phase}) = (\sigma(y) \cdot 2\pi/\lambda)^2 .$$

Consequently, as shown in Eq. A36 of App. A, the effect on P can be obtained from

$$P = \sum_{k=1}^N A_k^2 B_k^2 + 2 \sum_{i=1}^{N-1} \sum_{k=1}^{N-i} A_k B_k A_{k+i} B_{k+i} (1 - \text{VAR}(\text{phase})) \cdot \cos(\theta_k - \theta_{k+i}) . \quad (\text{Eq. 7})$$

1.4.2 Effect of Deterministic Placement Errors

As outlined earlier, these are positional errors, and consequently phase errors, that are caused by the synthesizing array following an oscillating course around an assumed straight-line course.

A phase error is introduced (see App. A, Sect. A4.2) because the actual ranges for the steering and delay vectors are different from those that were assumed. The result is that the ranges R_{S_i} and R_{S_k} defined in App. A must be modified by the across-track and along-track displacements of the synthesizing array from the assumed positions. The resulting equation for the synthesizing beam pattern, excluding all other errors, is given by Eq. A.44 of App. A.

$$P = \sum_{k=1}^N A_k^2 B_k^2 + 2 \sum_{i=1}^{N-1} \sum_{k=1}^{N-i} A_k B_k A_{k+i} B_{k+i} \cos(\theta_k' - \theta_{k+i}') \quad (\text{Eq. 8})$$

where θ_k' , θ_{k+i}' are the modified values obtained using Eqs. A.41, A.42 and A.43 of App. A.

1.5 Results

The results in Figs. 3 to 7 cover only the main lobe and nearby sidelobes of the synthesized beam. They are in a standardized form, independent of frequency, for a synthesized aperture (L) of 50λ with signal samples taken at 0.4λ spacing (no diffraction lobes in real space for all angles of steer) and for an array speed along-the-track of $U = 2$ m/s. The sine of the steer angle covers the interval ± 0.1 and the sine of the 3 dB beamwidth is approximately ± 0.01 .

To relate the curves to a frequency we simply use the required value of λ to obtain L and consequently the value of U to obtain T_s and the sampling interval ($\Delta t = 0.4\lambda/U$). Thus a speed other than 2 m/s alters only the values of T_s and Δt .

For a synthesized aperture other than 50λ we alter appropriately the coordinate of the sine of the steer angle to cover the new range of angles, and adjust the vertical coordinate for the different value of gain. For example, with a 10λ array the coordinate of the sine of the steer angle becomes ± 0.5 and the vertical axis is reduced by $10 \log 5$. Additionally, the value of T_s is reduced.

1.5.1 Effect of Coherence Time

Figure 3 shows beam patterns plotted for different ratios of T_c/T_s where T_s is the synthesizing time. It is seen that, as modelled in this study, a value of T_c at least equal to or greater than T_s is necessary to retain a reasonable beam-pattern. Alternatively, T_s must be less than T_c . Reported values of T_c applicable to synthetic-aperture studies are difficult

to find in the literature; one appropriate set [14] for a 400 Hz signal spans values of 148 s for a range of 93 n.mi and 450 s for a range of 268 n.mi. Some propagation measurements under the ice in the Arctic [15] suggest that long coherence times can exist there.

1.5.2 Effect of Random Phase and Amplitude Errors

Figure 4 shows the results obtained by modelling random phase and amplitude errors as a function of the signal-to-noise power ratio (S/N) at the input to the beamforming process. Although the definitions of ξ and η are such that they can only show trends, they are not of an unreasonable magnitude. With these definitions, the results suggest that a S/N of at least 3 dB is required to maintain an acceptable mainlobe-to-sidelobe ratio. Alternatively, phase fluctuations of 0.11 of a cycle and amplitude fluctuations of 0.7 of the maximum (A) can be tolerated.

1.5.3 Effect of Deterministic Placement Errors

Figure 5 shows the effect of having a large take-off angle ($\gamma = 2^\circ$) for different ratios of T_s/T_0 where T_0 is the period of oscillation of the array. A large ratio is preferable; a value of 5 is about the lowest limit. Obviously the value of T_0 depends very much on how the synthesizing array is moved through the sea and consequently can be defined only for a particular system.

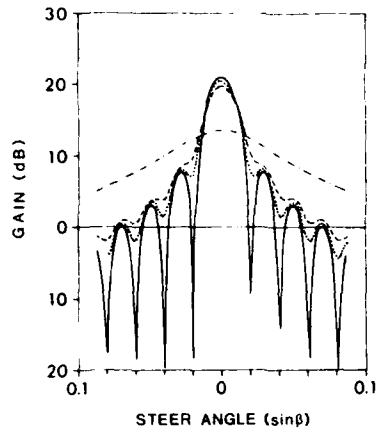
When the ratio T_s/T_0 is less than or equal to 0.1 an undistorted beam pattern is achievable but now a deflection of the main lobe occurs that approaches γ as T_s/T_0 is made smaller.

1.5.4 Effect of Random Placement Errors

As seen from Fig. 6 and as appreciated from the 'physics', a much larger random placement error can be tolerated as the frequency is reduced. Since, in general, random placement errors defined by a gaussian distribution with a standard deviation in excess of, say, 3 m are unlikely, the effect of this type of error could be made negligible by working at a sufficiently low frequency.

1.5.5 Effect of Weighting

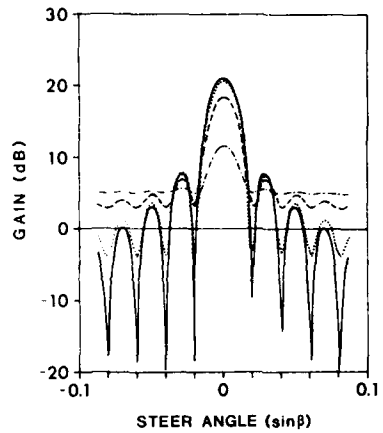
Two forms of array weighting have been evaluated to show the effect when deterministic errors are present. The results are shown in Fig. 7, in which the condition without weighting is for $\gamma = 2^\circ$ and for the worst-case ratio of $T_s/T_0 = 1$. Note that the Hamming weighting (controlled roll-off sidelobe levels) [16] gives a better result than the Dolph-Chebyshev weighting (constant value sidelobe levels) [17] in that the two peaks in the beam pattern are eliminated.



SA = 50λ, d = 0.4λ,
U = 2 m/s

T_c/T_s
0.1
1.0
2.0
∞

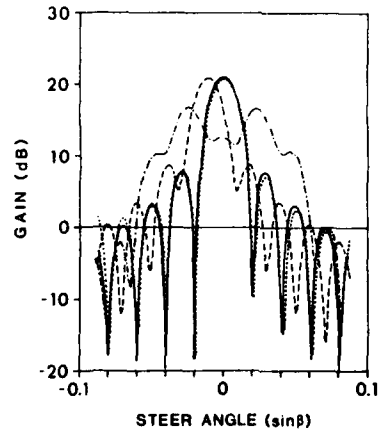
FIG. 3 EFFECT OF SIGNAL COHERENCE TIME



SA = 50λ ; d = 0.4λ ;
U = 2 m/s

S/N (dB)	$\sigma(\phi) / 2\pi$	$\sigma(a)$	T_E
∞	0	0	0
10.0	0.05	0.32	Δt
3.0	0.11	0.71	
0.5	0.15	0.95	

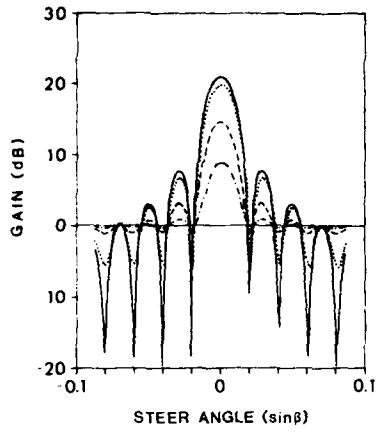
FIG. 4 EFFECT OF RANDOM PHASE AND AMPLITUDE ERRORS



SA = 50λ ; d = 0.4λ ;
U = 2 m/s

γ	T_S/T_0
0	∞
2.0°	5
	1
	0.1

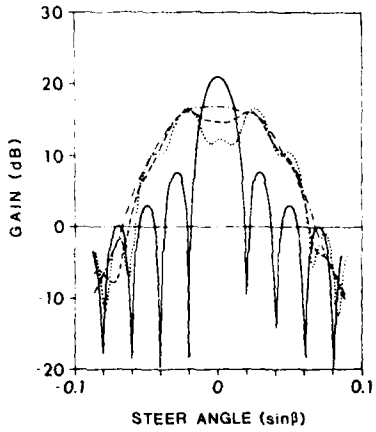
FIG. 5 EFFECT OF DETERMINISTIC PLACEMENT ERRORS



SA = 50λ ; d = 0.4λ ;
U = 2 m/s

	σ(y)	
	λ	σ(y)
—	0	0
.....	0.08	0.4m 2.0m
---	0.14	0.7m 3.5m
----	0.16	0.8m 4.0m

FIG. 6 EFFECT OF RANDOM PLACEMENT ERRORS



SA = 50λ ; d = 0.4λ ;
U = 2 m/s

	ERROR	WEIGHTING
—	none	none
.....	$\gamma = 2^*$ $T/T_0 = 1$	none
---	as above	Hamming
----	as above	Dolph-Chebyshev

FIG. 7 EFFECT OF 'WEIGHTING' IN THE PRESENCE OF DETERMINISTIC PLACEMENT ERRORS

2 ACTIVE SYNTHETIC-APERTURE PROCESSING

The system envisaged for active operation is one in which pulse transmissions are made successively as the synthesizing array is moved forward (see Fig. 8).

Transmission is made at periods corresponding to the assumed position of the target (stationary) with own-doppler nullification being carried out before the synthetic beamforming process. Consequently, the periods between the spatial samples are not equal, although for far-field beamforming the difference is very small. The time between transmission is dependent on the maximum range of interest but is usually severely constrained by the spatial sampling conditions. Transmission and reception must be made at least at every half-wavelength travelled in order to avoid diffraction lobes. This sampling distance can be increased (in practical cases) to almost a wavelength, since in general only small angles of steer are used. Thus, for these conditions the maximum range (R) of operation is given by:

$$R_{\max} = \frac{1}{2} \left(\frac{c\lambda}{U} \right) \quad (\text{Eq. 9})$$

For a frequency of 300 Hz and a platform speed U of 2.5 m/s the maximum range of operation is approximately 3 km. This is a severe limitation, but can be extended by using a physical array beam pattern with nulls in the direction of the likely diffraction lobes caused by under sampling when using a longer range. Alternatively, a lower frequency, increases the operating range.

The model also allows for specific complex weighting functions to be introduced to shape and steer the synthesized beam. The synthesized beam patterns are calculated for an ideal straight-line course of the synthesizing array and also for the more realistic case of a non-linear course. A sinusoidal course is actually considered in the model. The effect of random positional errors on the beamforming process is also considered. In addition, an attempt is made to include the effect of random fluctuations in the amplitude and in the phase of the received echoes. The procedure followed is similar to that used by the present authors in a first study on synthetic aperture [18].

2.1 Active Idealized Beamforming

The main assumption for the active mode of ideal operation is that the phase of the received echoes can be derived from geometrical considerations. This is equivalent to saying that the received echoes are not distorted on reflection from the target by multipaths, by phase fluctuations during propagation, or by a low signal-to-noise ratio.

The geometry of the synthesizing sequence is shown in Fig. 8. The synthesized beam will be steered and focussed to the target, which is assumed stationary. The mathematical derivation of active beamforming is developed in App. B.

PRECEDING PAGE BLANK-NOT FILMED

To form a synthesized beam we sum N samples of the received echoes S_k weighted by the appropriate delay and steering vectors of component d_k (see App. B):

$$V(\beta_T) = \sum_{k=1}^N s_k \cdot d_k \cdot w_k \quad , \quad (\text{Eq. 10})$$

where w_k is the amplitude weighting function to shape the beam, or in the complex form:

$$V(\beta_T) = \sum_{k=1}^N S_k \quad . \quad (\text{Eq. 11})$$

By varying the bearing β_T of T it will be possible to trace out the synthesizing beam pattern. An estimate of the resulting beam-power output in function of β_T and for a fixed β_A is given by:

$$P(\beta_T) = E\{V(\beta_T) \cdot V^*(\beta_T)\} \quad . \quad (\text{Eq. 12})$$

Then the beam power is:

$$P(\beta_T) = \left[\sum_{k=1}^N R_e(S_k) \right]^2 + \left[\sum_{k=1}^N I_m(S_k) \right]^2 \quad . \quad (\text{Eq. 13})$$

In App. B we show that when the ratio of R_0 to the synthesized aperture length is much larger than unity and with uniform amplitude weighting of the sampled echoes, the power beam pattern is given by the far-field beam pattern of the familiar form $(\sin(Nx)/\sin(x))^2$ [19]. We also show that the 3-dB beamwidth of the active synthetic-aperture array is one-half that of the passive array of the same aperture. This important result can be explained from the mode of operation of synthetic aperture. In fact, the essential feature of the synthetic-aperture technique is that signals are transmitted at successive positions of the array and each corresponding echo is delayed by a two-way path, and that the corresponding phase-shift is also twice that experienced in normal array operation. Consequently, after processing of the echoes the resulting beam pattern has a 3 dB beamwidth, which is half of that of a physical array of the same effective total length (Fig. 9).

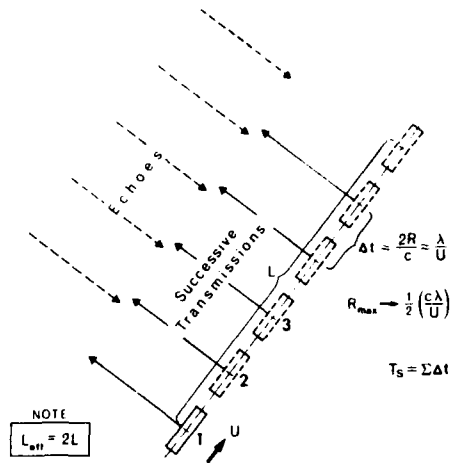


FIG. 8 SAS - ACTIVE MODE

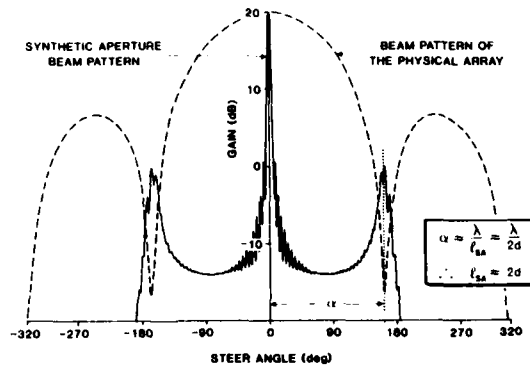


FIG. 9 REDUCTION OF UNDERSAMPLING SIDELOBES BY USING THE BEAM PATTERN OF THE PHYSICAL ARRAY

To calculate $P(\beta_T)$ we take the amplitude weighting function:

$$W(k) = B(k) \cdot b(k) \quad , \quad (\text{Eq. 14})$$

where

$$B(k) = f(\alpha_k) \cdot f(r_k) \quad . \quad (\text{Eq. 15})$$

The function $f(\alpha_k)$ is the amplitude response pattern of the synthesizing array. In our computer model we have taken:

$$f(\alpha_k) = \frac{\sin(n x_k)}{\sin(x_k)} \quad , \quad (\text{Eq. 16})$$

where n = number of hydrophones

$$\text{and } x_k = \frac{\pi d}{\lambda} \sin \alpha_k \quad , \quad (\text{Eq. 17})$$

with

d = separation between transducers
 λ = wavelength
 α = angle (from broadside) at which the target is seen by the physical array.

The coefficient $b(k)$ is an amplitude weighting factor that can be used to shape the synthesized beam pattern. Our model uses a weighting "Hamming" function

2.2 Effect of Random Amplitude & Phase Errors

The effect of random amplitude and phase errors on active beamforming are evaluated under the same assumptions given in Sect. 1.3 for the case of passive beamforming. The beam pattern synthesized by active mode of operation is calculated with the amplitude term $W(k)$ and phase term of S_k given by:

$$\tilde{W}(k) = W(k) + \eta(k) \quad (\text{Eq. 18})$$

$$\tilde{\gamma}(k) = \theta_{kT} + \varepsilon_{kT} \quad , \quad (\text{Eq. 19})$$

where

$W(k)$ = amplitude with no fluctuations
 $\eta(k)$ = random fluctuation in the amplitude
 θ_{kT} = phase with no fluctuations
 ε_{kT} = random fluctuation in the phase.

For $\eta(k)$ and ε_{kT} we have assumed the same type of random process described in Ch. 1 for passive sonar.

2.3 Effect of Placement Errors

2.3.1 Effect of Deterministic Placement Errors

To analyze the deterministic placement errors in active beamforming we consider the same oscillatory course of the synthesizing element as for the passive mode of operation (see Ch. 1).

The path geometry in the active case is shown in Fig. 10. The error produced in the phase θ_{kT} of the received echo S_k is given by:

$$\psi_{kT} = \frac{2\pi f_0}{c} (r'_{kT} + r''_{kT}) - (R'_{kT} + R''_{kT}) \quad , \quad (\text{Eq. 20})$$

where

- f_0 = frequency of the signal
- c = speed of sound
- r', r'' = distance of the oscillating synthesizing element from the target
- R', R'' = distances of the synthesizing element from the target in the case of straight-line course

Based on the geometry of Fig. 10, we calculate the distances r' and r'' in terms of the same oscillatory-course parameters (i.e. speed along the course, maximum off-track angle, period of oscillation) used in the passive case. A detailed mathematical analysis of the phase error ψ_{kT} in terms of the path geometry described above is given in App. B.

The synthesized beam pattern in presence of placement errors is calculated from Eq. 12, in which the phase θ_{kT} is replaced by the sum:

$$\tilde{\theta}_{kT} = \theta_{kT} + \psi_{kT} \quad , \quad (\text{Eq. 21})$$

where

- θ_{kT} = ideal phase term for straight-line course
- ψ_{kT} = phase error term given by Eq. 20.

2.3.2 Effect of Random Placement Errors

Superimposed on the deterministic errors we have assumed that other placement errors are caused by random fluctuations in the motion of the synthesizing array. For instance, a cause of random error can be the random fluctuation of the velocity of the synthesizing array. These random placement errors have been characterized by a circular gaussian distribution so that the standard deviation is the same for all signal directions. The variance of the corresponding phase error of the signal is given by:

$$\phi^2 = \left(\sigma_y \cdot \frac{2\pi}{\lambda}\right)^2 \quad ,$$

where λ is the wavelength of the signal and σ_y is the standard deviation of errors distribution.

2.4 Simulation Results

Figure 11 shows the result of an active synthetic-aperture technique working at 100 Hz in the near-field. The range $R = 750$ m implies a sampling interval of about $\Delta t \sim 2R/C \sim 1$ s. Taking $U = 2$ m/s for the speed of the synthesizing array, the corresponding spacing d is equal to $U\Delta t \sim 2$ m. This spacing of 0.4λ at 300 Hz is adequate to avoid grating lobes in the total 180° arc. The resulting synthetic aperture has a total effective length of $L = U_s U = 400$ m. The beamwidth of the passive array of the same length is given by

$$\theta(3 \text{ dB}) = \frac{\lambda}{L} = \frac{5}{400} \text{ radians} \times 57.3 \frac{\text{degrees}}{\text{radian}} \approx 0.7^\circ$$

However, the 3-dB beamwidth computed from the curve in Fig. 11 is about 0.35° . This result shows an important feature of the synthetic-aperture technique, namely that the synthetic-aperture beamwidth is half the beamwidth (see Sect. 2.1) of a passive linear array of the same length. This result also differs from what we would obtain from a "normal" active array, which has a beamwidth that is about forty percent (40%) greater than that achieved by the active synthetic-aperture array.

Figure 12 shows that an adequate beam pattern can be obtained at a longer range of 15 km at a lower frequency ($f = 100$ Hz). Samples are taken at intervals of $\Delta t \sim 20$ s over a total synthesizing time of $T_s = 600$ s. An effective synthetic aperture of 1200 m, with $U = 2$ m/s, is therefore generated. The 3 dB beamwidth is 0.3° .

Figures 13 and 14 show the effects of 'deterministic' placement errors on active beamforming for 300 Hz and 100 Hz operating frequencies respectively. At 300 Hz there is a broadening effect on the main lobe; at 100 Hz a double-peak effect occurs. It appears that the effect of deterministic placement errors is more severe on active beamforming than on passive, since the active performance is acceptable for values of $\gamma < 0.5^\circ$ whereas values of $\gamma < 2^\circ$ can be tolerated in the passive mode.

This could be explained by the fact that there are two errors in determining the position of the array when in the active mode: one at the time of transmission and the other at reception of the echo.

The effects of weighting (Hamming) in the presence of the deterministic placement errors are presented in Figs. 15 and 16 for $f = 300$ Hz and 100 Hz respectively. In both cases the weighting function smooths out all distortions in the beam pattern. It is noticeable that with $f = 100$ Hz the weighting also improves bearing resolution.

The effect of signal-to-noise ratio on active synthetic aperture has also been investigated. The results are very similar to those obtained for the passive mode (see Fig. 1) in which side lobes of the beam pattern are increased at low signal-to-noise ratios.

A beam pattern with acceptable main-lobe/sidelobe ratio was obtained in the active mode for a signal-to-noise ratio not lower than 3 dB.

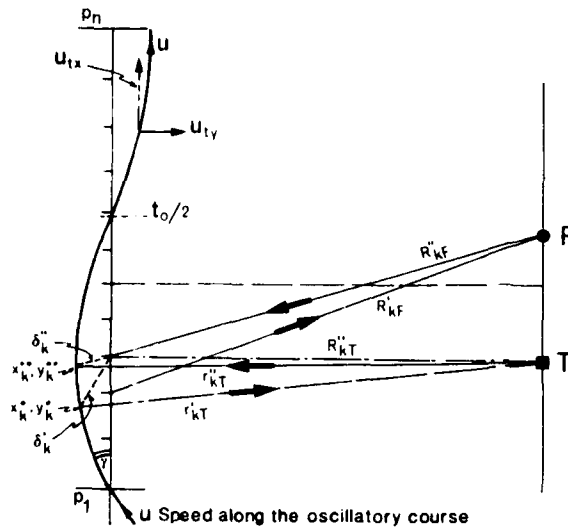


FIG. 10 GEOMETRY OF THE OSCILLATING COURSE

FIG. 11
ACTIVE SAS - SYNTHESIZED BEAMPATTERN
(No placement errors, high S/N ratio)

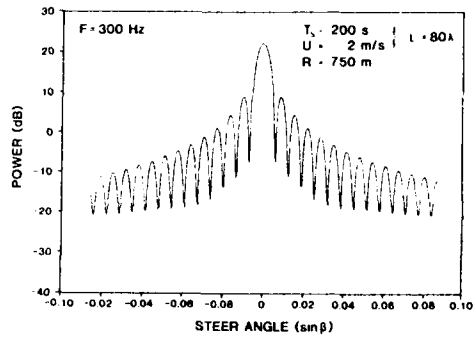
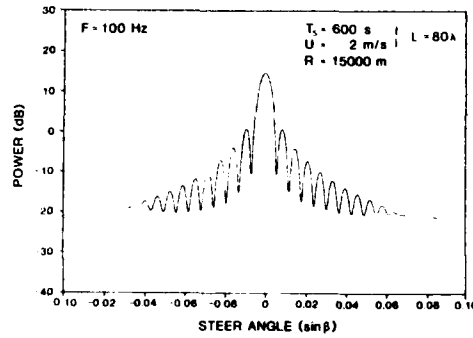


FIG. 12
ACTIVE SAS - SYNTHESIZED BEAMPATTERN
(No placement errors, high S/N ratio)



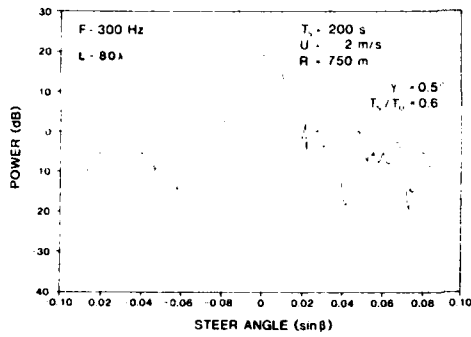


FIG. 13
ACTIVE SAS - EFFECT OF
DETERMINISTIC PLACEMENT
ERRORS

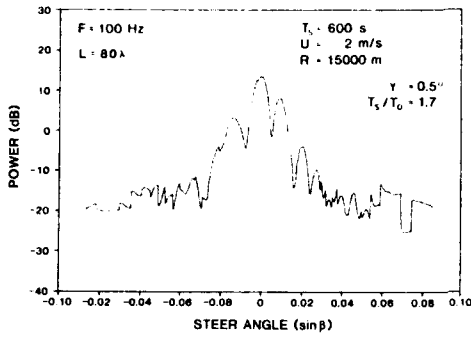


FIG. 14
ACTIVE SAS - EFFECT OF
DETERMINISTIC PLACEMENT
ERRORS

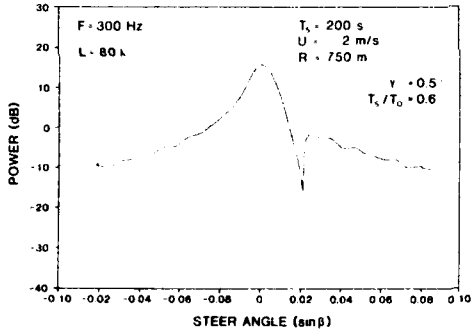


FIG. 15
ACTIVE SAS - EFFECT OF
WEIGHTING IN PRESENCE OF
DETERMINISTIC PLACEMENT
ERRORS (Hamming weighting)

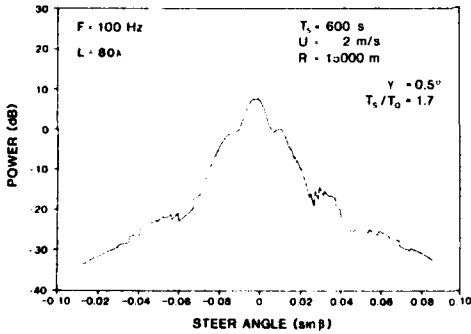


FIG. 16
ACTIVE SAS - EFFECT OF
WEIGHTING IN PRESENCE OF
DETERMINISTIC PLACEMENT
ERRORS (Hamming weighting)

CONCLUSIONS

The results obtained from computer simulations of the synthetic aperture techniques as applied to passive sonar, indicate that the following points need consideration in designing a passive synthetic-aperture sonar system:

- Signal coherence time must be long, or at least equal to the total synthesizing time necessary to form a synthetic aperture.
- Signal-to-noise ratio at the output of the synthesizing array must be larger than 3 dB (see para 1.5.2).
- 'Deterministic' placement errors caused by the movement of the towing vessel allow acceptable beamforming performance if the take-off angle of the track is not larger than 2° and the total synthesizing time is at least five times longer than the period of 'oscillation' of the vessel around its nominal straight course.
- Random placement errors caused by the fluctuations in the motion of the synthesizing array can be tolerated if the standard errors are less than 0.16 .
- Weighting (Hamming) can reduce the effect of placement errors on the synthesized beam pattern.

The simulation of active synthetic aperture indicates that the following points must be considered in designing an active synthetic-aperture sonar system:

- Maximum operating range is limited but can be increased by lowering the frequency. Moderate ranges of 10 to 15 km can be achieved at a frequency of the order of 100 Hz. Lower frequencies may require long synthesizing arrays. Higher frequencies may cause diffraction lobes in the synthesized beam pattern at the ranges considered.
- As in the passive mode, a signal-to-noise ratio of 3 dB at the output of the physical array appears adequate for beamforming.
- The effects of placement errors is more pronounced than in the passive mode.
- Weighting (Hamming) minimizes the effects of placement errors.
- The angular reflections of scatterers must be coherent during the synthesizing time.

These results indicate that the coherence time of the signal is likely to be the major problem in the passive mode if large synthetic apertures are required at low speeds. For a fixed synthetic-aperture length an increase in speed reduces the total synthesizing time and consequently a shorter coherence time is required. We suggest that passive sonar should make more use of the temporal coherence of a signal. The synthetic-aperture technique looks for long coherence times; perhaps the first step is to seek small improvements in aperture length.

The main requirement for the good performance of an active synthetic-aperture system is that the angular reflection characteristics of the scatterers remain coherent throughout the synthesizing time.

In the passive mode there is no limit on operating rate, because the sampling time is not range dependent as it is in the active case. The operating range for an active synthetic aperture can be extended by lowering the frequency.

Low signal-to-noise ratios, as modelled in this work, have little effect on the bearing resolution achievable, either with passive or active synthetic-aperture systems. A 3 dB signal-to-noise ratio at the input of the beamformer appears adequate for both passive and active systems.

The random placement errors can be made negligible by operating at low frequencies. The 'deterministic' errors can considerably affect the performance of a synthetic-aperture system if the take-off angles of the moving array are larger than 2° in the passive mode and larger than 0.5° in the active.

One very important conclusion of this study is that there is no experimental information in the open literature on which to base an accurate evaluation of the performance that could be achieved with an actual system. Measurements are required that are directly applicable to the synthetic-aperture technique. Consequently they must be made with a moving receiver platform and at various sampling times. Ultimately the movement of the source must be included.

REFERENCES

1. CUTRONA, L.S., VIVIAN, W.E., LEITH, E.N. and HALL, G.O. A high-resolution combat-surveillance system. IRE Transactions on Military Electronics, 5, 1961: 127-130.
2. SHERWIN, C.W., RUINA, J.P. and RAWCLIFFE, R.D. Some early developments in synthetic aperture systems. IRE Transactions on Military Electronics, 6, 1962: 111-115.
3. BUCKNAM, J.N., CHWASTYK, A.M., BLACK, H.D. and PADDISON, F.C. Synthetic aperture sonar, Technical memorandum TG 1161 A. Silver Spring, M.D., the Johns Hopkins University, Applied Physics Laboratory, 1971. [AD 744 657]
4. SATO, T., UEDA, M. and FUKUDA, S. Synthetic aperture sonar. Journal of the Acoustical Society of America, 54, 1972: 799-802.
5. CUTRONA, L.J. Comparison of sonar system performance achievable using synthetic-aperture techniques with the performance achievable by more conventional means. Journal of the Acoustical Society of America, 58, 1975: 336-348.
6. LOGGINS, C.D. Synthetic aperture sonar theory and system design. Journal of the Acoustical Society of America, 72, 1982: S73 PP6.
7. DE HEERING, P. Suboptimal processing in synthetic aperture sonar. In: GROUPE D'ETUDE DU TRAITEMENT DU SIGNAL. Neuvième Colloque sur le traitement du signal, Nice, 16-20 mai, 1983. Nice, GRETSI, 1983: pp. 679-684.
8. HEIMILLER, R.C. Theory and evaluation of gain patterns of synthetic arrays, IRE Transactions on Military Electronics, 6, 1962: 122-129.
9. GREEN, C.A. and MOLLER, R.T. The effect of normally distributed random phase errors on synthetic array gain patterns, IRE Transactions on Military Electronics, 6, 1962: 130-139.
10. LEE, H.E. Extension on synthetic aperture radar (SAR) Technique to undersea applications. IEEE Journal of Oceanic Engineering, 4, 1979: 60-63.
11. CUTRONA, L.J. Additional characteristics of synthetic-aperture sonar systems and a further comparison with non-synthetic-aperture sonar systems. Journal of the Acoustical Society of America, 61, 1977: 1213-1217.
12. SATO, T. and IKEDA, O. Sequential synthetic aperture sonar systems-prototype of synthetic aperture sonar system. IEEE Transactions on Sonics and Ultrasonics, 24, 1977: 253-259.

13. PUSONE, E. and LLOYD, L. Passive synthetic aperture sonar - an analysis of the beamforming process. In: URBAN, H.G. Proceedings of the NATO Advanced Study Institute on Adaptive Methods in Underwater Acoustics, Lüneburg, (FRG), August, 1984. Dordrecht, Reidel, 1985.
14. WILLIAMS, R.E. Creating an acoustic aperture in the ocean. Journal of the Acoustical Society, 60, 1976: 60-73.
15. DI NAPOLI, F.R., NIELSE, R., POTTER, D. and STOCKLIN, P.L. TRISTEN/FRAM IV CW spatial coherence and temporal stability. NUSC TD 7095. New London, CT, Naval Underwater Systems Center, 1984.
16. BLACKMAN, R.B. and TURKEY, J.W. The Measurement of Power Spectra. New York, NY, Dover, 1959.
17. SKOLNIK, M.I. Introduction to Radar Systems. New York, NY, McGraw-Hill, 1962.
18. PUSONE, E. and LLOYD, L. Synthetic aperture sonar: an analysis of beamforming and system design. In: INSTITUTE OF ELECTRICAL AND ELECTRONICS ENGINEERS. ACOUSTICS, SPEECH, AND SIGNAL PROCESSING SOCIETY. IEEE International Conference on Acoustics, Speech, and Signal Processing, ICASSP 84, March 19-21, 1984, San Diego, California. Piscataway, N.J., IEEE, 1984: Vol. 2: pp. 33.12.1 to 33.12.4.
19. KING, R.W.P. The Theory of Linear Antennas. Cambridge, MA, Harvard University Press, 1956.

APPENDICES

APPENDIX A

MATHEMATICAL DESCRIPTION OF THE PASSIVE
SYNTHETIC-APERTURE BEAMFORMING PROCESS

In the passive synthetic-aperture beamforming process, samples of the signal received at successive positions of the synthesizing array as it moves through the synthesizing sequence are compensated for the delay time between samples and the movement of the array and then added coherently. The prediction of performance is obviously very dependent on the following assumptions:

- a. The radiating source is stationary and radiates with a constant amplitude and phase.
- b. Own-doppler nullification (ODN) is carried out on the received signals before commencing the synthetic-aperture beamforming process.

We start by analyzing the idealized case, in which it is assumed that the signal field is perfectly coherent in space and time during the synthesizing period (T_s) and that the synthesizing array moves along a perfectly straight course at a known constant speed. Hereafter we examine the effect of:

- a. The temporal signal coherence not being perfect but being characterized by a coherence time (T_c).
- b. Random phase and amplitude errors in the signals received at successive positions of the synthesizing array.
- c. Random and deterministic errors in the position of the synthesizing array as it moves through the synthesizing sequence.

A.1 IDEALIZED BEAMFORMING

On the basis of the assumptions given above, the geometry of the synthesizing sequence is as shown in Fig. A1. The delay and steering vectors required to focus the successive signals to F (the assumed position of the source) can be derived by first considering the received phase of a signal radiating from F and then reversing this phase. The phase of the signal received at the start of the synthesizing sequence is taken as a reference.

Using the geometry of Fig. A1, the phase of the k^{th} signal received from F is:

$$\phi_{Fk} = \omega\{t_1 - (k-1)\Delta t + (R_{Fk} - R_{F1})/c\} , \quad (\text{Eq. A.1})$$

where ωt_1 is the reference phase. Consequently the delay and steering vectors are given by

$$d_k = A_k \exp[-j\omega\{t_1 - (k-1)\Delta t + (R_{Fk} - R_{F1})/c\}] , \quad (\text{Eq. A.2})$$

where A_k is an amplitude-weighting function that can be used to shape the synthesized beam pattern if required.

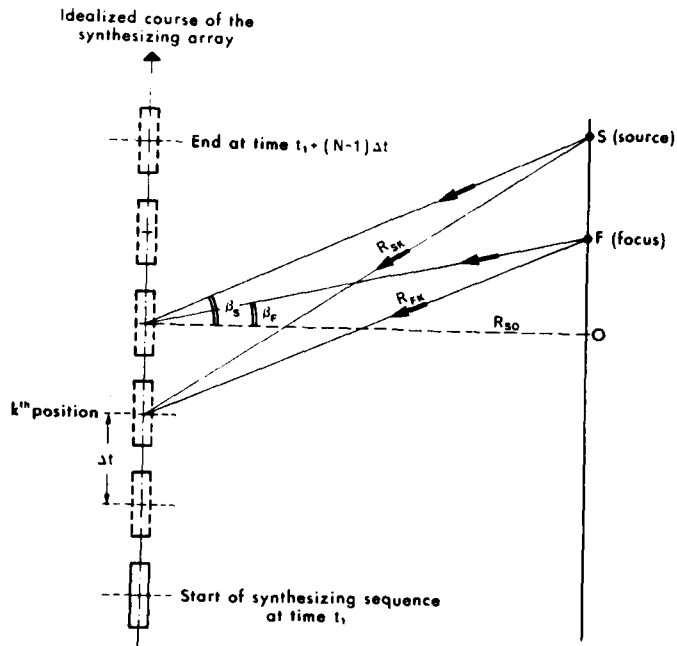


FIG. A1 GEOMETRY FOR PASSIVE SYNTHETIC APERTURE MODE
 Initial values of R_{SK} and R_{FK} are R_{S1} and R_{F1} respectively.

APPENDIX A

MATHEMATICAL DESCRIPTION OF THE PASSIVE
SYNTHETIC-APERTURE BEAMFORMING PROCESS

In the passive synthetic-aperture beamforming process, samples of the signal received at successive positions of the synthesizing array as it moves through the synthesizing sequence are compensated for the delay time between samples and the movement of the array and then added coherently. The prediction of performance is obviously very dependent on the following assumptions:

- a. The radiating source is stationary and radiates with a constant amplitude and phase.
- b. Own-doppler nullification (ODN) is carried out on the received signals before commencing the synthetic-aperture beamforming process.

We start by analyzing the idealized case, in which it is assumed that the signal field is perfectly coherent in space and time during the synthesizing period (T_s) and that the synthesizing array moves along a perfectly straight course at a known constant speed. Hereafter we examine the effect of:

- a. The temporal signal coherence not being perfect but being characterized by a coherence time (t_c).
- b. Random phase and amplitude errors in the signals received at successive positions of the synthesizing array.
- c. Random and deterministic errors in the position of the synthesizing array as it moves through the synthesizing sequence.

A.1 IDEALIZED BEAMFORMING

On the basis of the assumptions given above, the geometry of the synthesizing sequence is as shown in Fig. A1. The delay and steering vectors required to focus the successive signals to F (the assumed position of the source) can be derived by first considering the received phase of a signal radiating from F and then reversing this phase. The phase of the signal received at the start of the synthesizing sequence is taken as a reference.

Using the geometry of Fig. A1, the phase of the k^{th} signal received from F is:

$$\phi_{FK} = \omega\{t_1 - (k-1)\Delta t + (R_{FK} - R_{F1})/c\} \quad (\text{Eq. A.1})$$

where ωt_1 is the reference phase. Consequently the delay and steering vectors are given by

$$d_k = A_k \exp[-j\omega\{t_1 - (k-1)\Delta t + (R_{FK} - R_{F1})/c\}] \quad (\text{Eq. A.2})$$

where A_k is an amplitude-weighting function that can be used to shape the synthesized beam pattern if required.

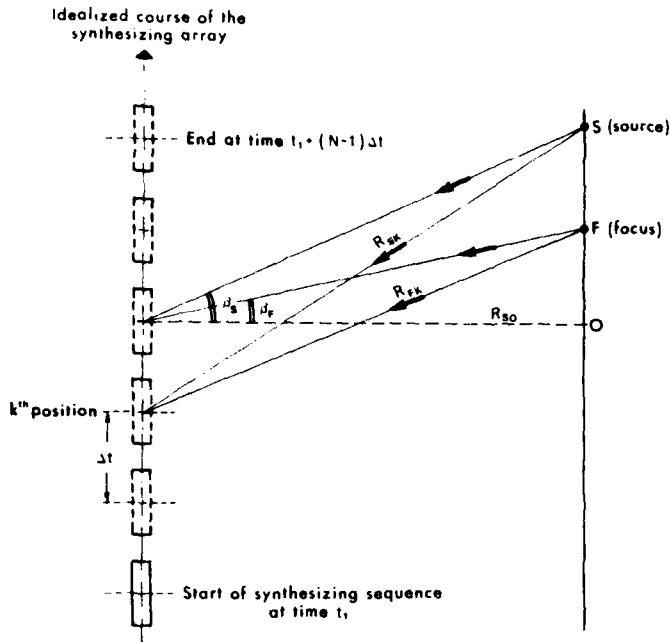


FIG. A1 GEOMETRY FOR PASSIVE SYNTHETIC APERTURE MODE
 Initial values of R_{SK} and R_{FK} are R_{S1} and R_{F1} respectively.

The next step is to define the signals received from a source not positioned at F to which the above vectors will be applied. By varying the bearing of this source it will be possible to trace out the synthesized beam pattern.

From Eq. A.1, the k^{th} signal sample obtained from a source at position S (see Fig. A1) is given by:

$$s_k = B_k \exp[j\omega\{t_1 - (k-1)\Delta t + (R_{Sk} - R_{S1})/c\}] \quad (\text{Eq. A.3})$$

In this expression B_k is introduced to allow for the signal amplitude (b_k) and for the amplitude response of the receiving array in the direction of S, and to normalize the amplitude levels relative to the amplitude received when s lies on the broadside axis of the synthetic aperture. Thus:

$$B_k = b_k f(\alpha_S) \cdot f(R_S) ,$$

where $f(\alpha_S)$ is the amplitude response pattern of the physical array (a function of the number of hydrophones, spacing, and shading function of the physical array), and $f(R_S)$ is R_{S0}/R_{Sk} . This latter factor is consequently 1 when the source is on the broadside axis; otherwise it is less than 1.

As stated previously, to derive Eq. A.3, we assume that own-doppler nullification has been carried out before the synthetic beamforming process starts. However, the own-doppler nullification will be correct only for signals from the focus, since this is the direction from which it is assumed the signals are arriving. Thus the present analysis makes no allowance for the actual doppler differing from the assumed value as the position of the source is varied to generate the synthesized beam pattern.

To form a synthesized beam we sum N samples of the received signals, with the appropriate delay and steering vectors being applied. Using Eqs. A.2 and A.3 the beam output voltage is given by:

$$V(\beta) = \sum_{k=1}^N s_k \cdot d_k = \sum_{k=1}^N S_k \quad (\text{Eq. A.4})$$

Thus

$$V(\beta) = \sum_{k=1}^N A_k B_k \exp[j(\theta_{Sk} - \theta_{Fk})] \quad (\text{Eq. A.5})$$

where

$$\theta_{Sk} = (R_{Sk} - R_{S1})\omega/c \quad (\text{Eq. A.6})$$

$$\theta_{Fk} = (R_{Fk} - R_{F1})\omega/c \quad (\text{Eq. A.7})$$

Then in the usual manner we can write for the beam output power:

$$P = E\{V \cdot V^*\} = E\left\{ \left| \sum_{k=1}^N A_k B_k \cos(\theta_{Sk} - \theta_{Fk}) \right|^2 + \left| \sum_{k=1}^N A_k B_k \sin(\theta_{Sk} - \theta_{Fk}) \right|^2 \right\}$$

Since this contains no time-varying components we have:

$$P = \left| \sum_{k=1}^N A_k B_k \cos(\theta_{Sk} - \theta_{Fk}) \right|^2 + \left| \sum_{k=1}^N A_k B_k \sin(\theta_{Sk} - \theta_{Fk}) \right|^2 \quad (\text{Eq. A.8})$$

Referring back to Eq. 5 it can be seen from Fig. A.1 that:

$$R_{F1} = \left[(L/2 + R_0 \tan \beta_F)^2 + R_0^2 \right]^{1/2} \quad (\text{Eq. A.9})$$

$$R_{Fk} = \left[\{L/2 + R_0 \tan \beta_F - (k-1)U\Delta t\}^2 + R_0^2 \right]^{1/2} \quad (\text{Eq. A.10})$$

and that the equations for R_{S1} and R_{Sk} are exactly the same, with β_F being replaced by β_S .

Returning for a moment to the equation for $V(\beta)$, we have from Eqs. A.5, A.6 and A.7 that

$$V(\beta) = \sum_{k=1}^N A_k B_k \exp[j\{R_{Sk} - R_{S1} + R_{F1} - R_{Fk}\}\omega/c] \quad (\text{Eq. A.11})$$

Then using Eqs. A.9 and A.10, and the similar ones for R_S and R_{Sk} it can be shown after some tedious algebra that for $R_0 \gg L$, namely in the far-field of the synthesized aperture:

$$V(\beta) = \exp[j\frac{\omega L}{2c}(\sin \beta_F - \sin \beta_S)] \cdot \sum_{k=1}^N A_k B_k \cdot \exp[j\frac{\omega}{c}(k-1)U\Delta t(\sin \beta_F - \sin \beta_S)]$$

Consequently when $A_k = B_k = 1$ we have for P the following:

$$P = E\{V \cdot V^*\} = \left[\frac{\sin\{N \frac{\pi U \Delta t}{\lambda} (\sin \beta_F - \sin \beta_S)\}}{\sin\{\frac{\pi U \Delta t}{\lambda} (\sin \beta_F - \sin \beta_S)\}} \right]^2 \quad (\text{Eq. A.12})$$

This is the standard expression for the far-field beam pattern of a linear array of N hydrophones equally spaced at intervals of $U\Delta t$.

It is usual to normalize P by dividing it by N^2 , so that its maximum value is 1 when β_F equals β_k . However, for this present study the normalization has been done with respect to N only. Thus with $A_k = B_k = 1$ for all values of k , P_0 will have a maximum value of $10 \log N$ when β_F equals β_S .

A.2 EFFECT OF THE TEMPORAL COHERENCE OF THE RECEIVED SIGNAL

Equations A.3 and A.8 for the k^{th} signal sample and the synthesized beam power respectively are both based on the assumption that all the received signal samples, after phase correction for movement and time difference, are fully coherent. This means that the normalized temporal correlation, or coherence in our case of a narrowband signal, is 1 during the period T_S . Namely, that:

$$\frac{E\{S_k \cdot S_{k+i}^*\}}{[E\{S_k^2\} \cdot E\{S_{k+i}^2\}]^{1/2}} = \rho(S_t) = 1 \quad , \quad (\text{Eq. A.13})$$

where S_k, S_{k+i} are defined by Eqs. A.4, A.5, A.6 and A.7.

In order to examine the likely effect of a lack of coherence, we assume that there is an exponential decay with time of $\rho(S_t)$, as follows:

$$\rho(S_t)_{\text{actual}} = \rho(S_t) \cdot \exp[-|t_{k+i} - t_k|/T_c] \quad , \quad (\text{Eq. A.14})$$

where T_c is referred to as the coherence time of the signal.

In other words we have:

$$E\{S_k \cdot S_{k+i}^*\} = \overline{S_k \cdot S_{k+i}} \exp[-|t_{k+i} - t_k|/T_c] \quad . \quad (\text{Eq. A.15})$$

The equation for the synthesized beam output power is now:

$$E\left\{\left(\sum_{k=1}^N S_k\right) \cdot \left(\sum_{k=1}^N S_k\right)^*\right\} \quad ,$$

thus:

$$\begin{aligned} P &= \sum_{k=1}^N S_k^2 + 2 \sum_{i=1}^{N-1} \sum_{k=1}^{N-i} E\{S_k \cdot S_{k+i}^*\} \\ &= \sum_{k=1}^N S_k^2 + 2 \sum_{i=1}^{N-1} \sum_{k=1}^{N-i} \overline{S_k \cdot S_{k+i}} \exp[-|t_{k+i} - t_k|/T_c] \quad . \quad (\text{Eq. A.16}) \end{aligned}$$

A.3 EFFECT OF RANDOM PHASE AND AMPLITUDE ERRORS IN THE RECEIVED SIGNAL

Random fluctuations can occur in the amplitude and phase of the received signal due to a number of factors. Examples of some of these factors are fluctuations of the radiating source, fluctuations caused during the propagation of the signal, the presence of noise, and multipaths causing constructive and destructive interference along the synthesizing path.

It is not possible to characterize these fluctuations from the published information on fluctuations, because none of the information is strictly applicable to the synthetic-aperture technique. All the published information has been obtained with stationary receivers and some measurements were made with spaced receivers. However, these were simultaneous measurements and therefore not useful for synthetic-aperture studies.

Consequently, we base the following analysis on the assumption that such random errors can be studied by including random fluctuation components, η and ε , in the amplitude and phases respectively of the received signal. We further assume that η and ε are independent of each other and of the actual amplitudes and phases, and can be characterized as first-order Markov processes. Then in order to quantify the effect of these fluctuations (bearing in mind the lack of experimental data) their root mean square (rms) values have been related to the signal/noise ratio. The complete assumptions can be written as:

$$\overline{\eta_k^2} = \overline{\eta_{k+i}^2} \quad \text{noise power} \quad (\text{Eq. A.17})$$

$$E\{\eta_k \cdot \eta_{k+i}\} = \overline{\eta_k^2} \exp[-|t_{k+i} - t_k|/T_E] \quad (\text{Eq. A.18})$$

$$\overline{\varepsilon_k^2} = \overline{\varepsilon_{k+i}^2} (S/N)^{-1} \quad (\text{Eq. A.19})$$

$$\overline{\varepsilon_k} = 0$$

$$E\{\varepsilon_k \cdot \varepsilon_{k+i}\} = \overline{\varepsilon_k^2} \exp[-|t_{k+i} - t_k|/T_E] \quad (\text{Eq. A.20})$$

where

S/N = signal-to-noise power ratio at the output of the synthesizing array

T_E = correlation time for the amplitude and phase fluctuations, which are assumed to be equal.

As stated earlier, the need for the above assumptions highlights an area of considerable weakness in our knowledge of acoustic reception in the sea from a moving platform.

Using the above assumptions we can first rewrite Eq. A.8 for the power output of the synthesized beam as:

$$P = E\left\{\left[\sum_{k=1}^N A_k f(\alpha_k) f(R_k) \cdot (b_k + \eta_k) \cos(\theta_k + \varepsilon_k)\right]^2\right\} + E\left\{\left[\sum_{k=1}^N A_k f(\alpha_k) f(R_k) \cdot (b_k + \eta_k) \sin(\theta_k + \varepsilon_k)\right]^2\right\}. \quad (\text{Eq. A.21})$$

This can be put in the form of:

$$P = E\left\{\left[\sum_{k=1}^N r_k\right]^2\right\} + E\left\{\left[\sum_{k=1}^N p_k\right]^2\right\}, \quad (\text{Eq. A.22})$$

where

$$r_k = A_k f(\alpha_k) f(R_k) \cdot (b_k + \eta_k) \cdot \cos(\theta_k + \varepsilon_k), \quad (\text{Eq. A.23})$$

$$p_k = A_k f(\alpha_k) f(R_k) \cdot (b_k + \eta_k) \cdot \sin(\theta_k + \varepsilon_k) \quad (\text{Eq. A.24})$$

and

$$\theta_k = \theta_{S_k} - \theta_{F_k} \quad (\text{see Eqs. A.5 to A.8})$$

Equation A.21 can now be restructured to read:

$$P = \sum_{k=1}^N [E\{r_k^2\} + E\{p_k^2\}] + 2 \sum_{i=1}^{N-1} \sum_{k=1}^{N-i} [E\{r_k \cdot r_{k+i}\} + E\{p_k \cdot p_{k+i}\}] \quad (\text{Eq. A.25})$$

From Eqs. A.23 and A.24 the first summation in Eq. A.25 becomes:

$$\sum_{k=1}^N E\{[A_k f(\alpha_k) f(R_k) (b_k + \eta_k)]^2\}, \quad (\text{Eq. A.26})$$

which we will write as:

$$\sum_{k=1}^N q_k^2. \quad (\text{Eq. A.27})$$

Similarly,

$$E\{r_k \cdot r_{k+i}\} = q_k \cdot q_{k+i} [E\{\cos(\theta_k + \varepsilon_k) \cos(\theta_{k+i} + \varepsilon_{k+i})\}] \quad (\text{Eq. A.28})$$

Thus Eq. A.25 becomes

$$P = \sum_{k=1}^N q_k^2 + 2 \sum_{i=1}^{N-1} \sum_{k=1}^{N-i} q_k q_{k+i} [E\{\cos(\theta_k + \varepsilon_k) \cdot \cos(\theta_{k+i} + \varepsilon_{k+i})\} + E\{\sin(\theta_k + \varepsilon_k) \cdot \sin(\theta_{k+i} + \varepsilon_{k+i})\}] \quad (\text{Eq. A.29})$$

Using standard trigonometric relationship this becomes:

$$P = \sum_{k=1}^N q_k^2 + 2 \sum_{i=1}^{N-1} \sum_{k=1}^{N-i} q_k q_{k+i} [\cos(\theta_k - \theta_{k+i})] \cdot [E\{\cos(\varepsilon_k - \varepsilon_{k+i})\} - \sin(\theta_k - \theta_{k+i}) \cdot E\{\sin(\varepsilon_k - \varepsilon_{k+i})\}] \quad (\text{Eq. A.30})$$

Then, using the following approximations on the basis of small errors:

$$E\{\sin(\varepsilon_k - \varepsilon_{k+i})\} \approx E\{\varepsilon_k - \varepsilon_{k+i}\} = 0$$

$$E\{\cos(\varepsilon_k - \varepsilon_{k+i})\} \approx E\left\{1 - \frac{(\varepsilon_k - \varepsilon_{k+i})^2}{2}\right\} = 1 - E\{\varepsilon_k^2\} + E\{\varepsilon_k \cdot \varepsilon_{k+i}\} \quad .$$

The expression for P becomes:

$$P = \sum_{k=1}^N q_k^2 + 2 \sum_{i=1}^{N-1} \sum_{k=1}^{N-i} q_k q_{k+i} \cos(\theta_k - \theta_{k+i}) \cdot [1 - E\{\varepsilon_k^2\} + E\{\varepsilon_k \cdot \varepsilon_{k+i}\}] \quad (\text{Eq. A.31})$$

Referring back to Eqs. A.26 and A.27 we have:

$$q_k^2 = A_k^2 f^2(\alpha_k) f^2(R_k) \cdot (b_k^2 + \overline{\eta_k^2}) \quad (\text{Eq. A.32})$$

and thus:

$$q_k q_{k+i} = A_k f(\alpha_k) f(R_k) \cdot A_{k+i} f(\alpha_{k+i}) f(R_{k+i}) \cdot [E\{b_k \cdot b_{k+i}\} + E\{\eta_k \cdot \eta_{k+i}\}]$$

That is:

$$q_k q_{k+i} = A_k f(\alpha_k) f(R_k) \cdot A_{k+i} f(\alpha_{k+i}) f(R_{k+i}) \cdot [b_k^2 + \eta_k^2 \exp(-|t_{k+i} - t_k|/T_E)] \quad (\text{Eq. A.33})$$

Thus finally we have:

$$\begin{aligned}
 P = & \sum_{k=1}^N A_k^2 f^2(\alpha_k) f^2(R_k) (b_k^2 + \overline{\eta_k^2}) + \\
 & + 2 \sum_{i=1}^{N-1} \sum_{k=1}^{N-i} [A_k f(\alpha_k) f(R_k) \cdot A_{k+i} f(\alpha_{k+i}) f(R_{k+i}) \cdot \{b_k^2 + \\
 & + \overline{\eta_k^2} \exp(-|t_{k+i} - t_k|/T_E)] \cdot [1 - \overline{\epsilon_k^2} + \overline{\epsilon_{k+i}^2} \exp(-|t_{k+i} - t_k|/T_E)] \cos(\theta_k + \theta_{k+i}) \} \\
 & \hspace{15em} \text{(Eq. A.34)}
 \end{aligned}$$

A.4 EFFECT OF PLACEMENT ERRORS

The expression "placement error" is used to describe the difference in position between the actual and assumed positions of the synthesizing array as it moves through the synthesizing sequence. Such errors will cause the delay vectors to be incorrect. Thus, for example, a source at the "focus" of a synthesized aperture will not be focussed correctly. It should be noted, however, that since the degradation caused by these errors is obviously dependent on the ratio of the placement error to the wavelength in use, their effect can be reduced by reducing the operating frequency.

The present analysis attempts to simulate two types of placement error; Firstly, a purely random positional error, e.g. random navigational errors or an erratic movement of the synthesizing array through the sea and, secondly, a placement error caused by a non-linear track resulting from the oscillations of a moving platform about the desired straight course at sea. The second type of error is considered deterministic because the actual value of each successive error can be mathematically defined whereas the first type must be treated statistically.

A.4.1 The Effect of Random Placement Errors

The purely random placement errors are modelled by assuming a gaussian distribution of actual array positions about the assumed array position, with the errors being independent of each other and independent of the actual positions. The gaussian distribution is assumed to be circular, so that it produces the same effect for all signal directions. Thus it is defined by a single variance (σ_y^2) that can be converted to a variance in phase by:

$$\text{VAR (Phase)} = \left(\sigma_y \cdot \frac{2\pi}{\lambda} \right)^2 \quad \text{(Eq. A.35)}$$

Then, using Eq. A.34 and the assumptions outlined above, we obtain the analytical expression for the synthesized beam power output as:

$$P = \sum_{k=1}^N A_k^2 B_k^2 + 2 \sum_{i=1}^{N-1} \sum_{k=1}^{N-i} [A_k B_k A_{k+i} B_{k+i} \cdot (1 - \text{VAR}(\text{phase})) \cos(\theta_k - \theta_{k+i})] \quad (\text{Eq. A.36})$$

A.4.2 Effect of Deterministic Placement Errors

As stated earlier, the aim is to simulate the type of non-linear oscillating track that usually occurs at sea when a moving platform attempts to follow a straight-line course.

We therefore assume that the speed of the synthesizing array along the oscillating track is constant but not necessarily the assumed speed, and that the oscillation can be characterized by an across-the-track speed component of:

$$U_y(t) = U \sin \gamma \cdot \cos(2\pi t/T_0) \quad (\text{Eq. A.37})$$

where

- U = actual speed (constant) along the track
- γ = maximum off-track angle of the oscillating track.
- T_0 = period of the oscillation (see Fig. A1)

Thus for the along-track component of velocity we have:

$$U_x(t) = [U^2 - U_y^2(t)]^{1/2} = U [1 - \frac{\sin^2 \gamma}{2} \cos^2(2\pi t/T_0)]^{1/2} \quad (\text{Eq. A.38})$$

using the assumption that $\sin^2 \gamma \cdot \cos^2(2\pi t/T_0)$ is always $\ll 1$.

Consequently the deterministic placement errors are given by the displacement of the oscillating track from the nominal straight line, as follows:

$$\Delta x_k = \int_{TOS}^{T_k} U_x(t) \cdot dt \quad (\text{Eq. A.39})$$

$$\Delta y_k = \int_{TOS}^{T_k} U_y(t) \cdot dt$$

where

- T_k = time corresponding to the successive positions of the synthesizing array
- TOS = time corresponding to the initial position of the synthesizing array on the oscillating course.

The effect of these deterministic errors is then introduced by modifying in Eq. A.11 the values for the ranges R_{S1} and R_{Sk} (see Eqs. A.9 and A.10). Thus R_{S1} and R_{Sk} become:

$$R'_{S1} = [(L/2 + R_o \tan \beta_S)^2 + (R_o + \Delta y_1)^2]^{1/2} \quad (\text{Eq. A.40})$$

$$R'_{Sk} = [(L/2 + R_o \tan \beta_S - \Delta x_k)^2 + (R_o + \Delta y_k)^2]^{1/2} \quad (\text{Eq. A.41})$$

Therefore in the Eq. A.34 of P we will have

$$\theta'_k = \theta'_{Sk} - \theta_{Fk} \quad (\text{Eq. A.42})$$

$$\theta'_{k+i} = \theta'_{Sk+i} - \theta_{Fk} \quad (\text{Eq. A.43})$$

where θ'_{Sk} and θ'_{Sk+i} are obtained from Eqs. A.6 and A.7 using R'_{S1} and R'_{Sk} . So that with deterministic errors alone Eq. A.34 can be written:

$$P = \sum_{k=1}^N A_k^2 B_k^2 + 2 \sum_{i=1}^{N-1} \sum_{k=1}^{N-i} A_k B_k A_{k+i} B_{k+i} \cos(\theta'_k - \theta'_{k+i}) \quad (\text{Eq. A.44})$$

APPENDIX B

MATHEMATICAL DESCRIPTION OF THE ACTIVE BEAMFORMING PROCESS

ASSUMPTIONS

B.1 BEAMFORMING UNDER IDEAL CONDITIONS

The signal sequence transmitted by the synthesizing array ($s_1 s_2 \dots s_k \dots s_N$) and the corresponding echoes from focus F ($\tilde{s}_1 \tilde{s}_2 \dots \tilde{s}_k \dots \tilde{s}_N$) can be written in the forms:

$$s_k = \exp(j\omega t_k) \quad (\text{Eq. B.1})$$

$$\tilde{s}_k = a_k \exp \left[j\omega \left(t_k + \frac{R'_k + R''_k}{c} \right) \right] \quad (\text{Eq. B.2})$$

The geometry of transmission and reception is shown in Fig. B1.

The timing sequence is given by (see Fig. B2):

$$t_1 = \text{initial time of transmission}$$

$$t_2 = t_1 + \left(\frac{R'_1 + R''_1}{c} \right)_F + \tau \quad (\tau : \text{pulse length})$$

$$t_3 = t_2 + \left(\frac{R'_2 + R''_2}{c} \right)_F + \tau = t_1 + \left(\frac{R'_1 + R''_1}{c} \right)_F + \left(\frac{R'_2 + R''_2}{c} \right)_F + 2\tau \quad (\text{Eq. B.3})$$

⋮

$$t_k = t_1 + \sum_{k=1}^{k-1} (\Delta t)_{kF} + (k-1)\tau$$

⋮

$$t_N = t_1 + \sum_{k=1}^{N-1} (\Delta t)_{kF} + (N-1)\tau$$

where $\Delta t_{kF} = \left(\frac{R'_{kF} + R''_{kF}}{c} \right)$ as shown in Fig. B1.

PRECEDING PAGE BLANK-NOT FILMED

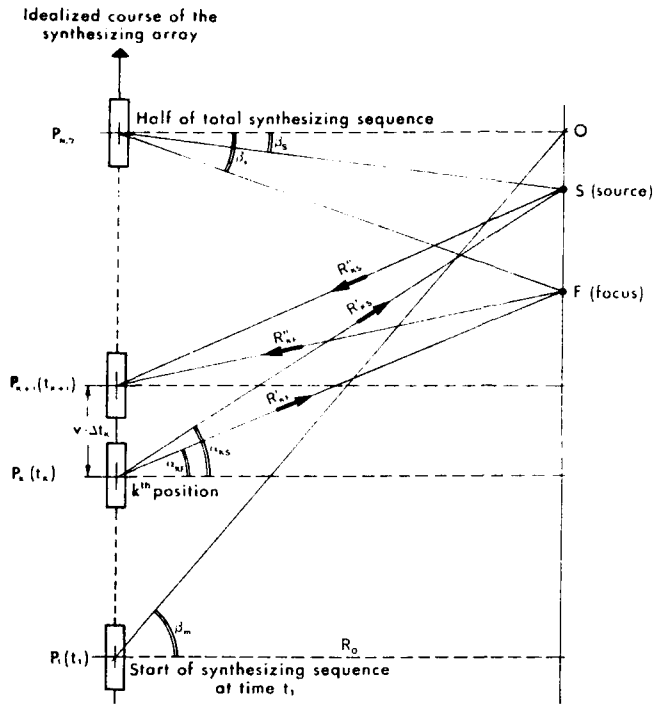


FIG. B1 GEOMETRY OF ACTIVE IDEAL BEAMFORMING

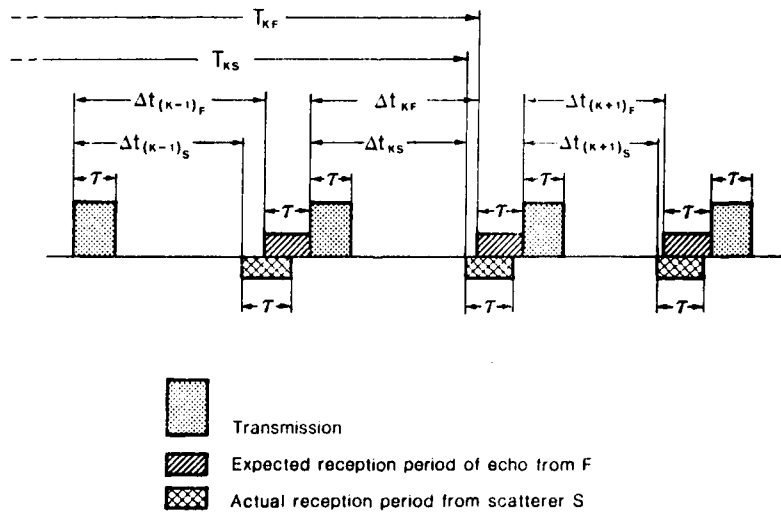


FIG. B2 TIMING SEQUENCE OF ACTIVE IDEAL BEAMFORMING

The k-th echo received from the focus F is given by:

$$\tilde{s}_k = a_k \cdot \exp\left\{j\omega\left[t_1 + \sum_{k=1}^{N-1} (\Delta t)_{kF} + (k-1)\tau\right] + (R'_{kF} + R''_{kF})/c\right\} \quad (\text{Eq. B.4})$$

or

$$\tilde{s}_k = a_k \cdot \exp\{j\omega(t_1 + T_{kF})\} \quad (\text{Eq. B.5})$$

To bring these signals into phase with the first received signal thus requires a steering vector of the form:

$$D_k = \exp(-j\omega T_{kF}) \quad , \quad (\text{Eq. B.6})$$

where

$$T_{kF} = \sum_{k=1}^N (\Delta t)_{kF} + (k-1)\tau \quad (\text{Eq. B.7})$$

The actual phase shift of the echo from the scatterer S relative to the first transmission ($t = t_1$) is given by:

$$r_k = b_k \cdot \exp\{j\omega(t_1 + T_{kS})\} \quad , \quad (\text{Eq. B.8})$$

where (see Fig. B2)

$$T_{kF} = T_{kS} + (\Delta t_{kF} - \Delta t_{kS}) \quad . \quad (\text{Eq. B.9})$$

To form beams we require:

$$V = \sum_{k=1}^N r_k \cdot D_k = \sum_{k=1}^N b_k \exp\{j\omega T_{kS}\} a_k \exp\{-j\omega T_{kF}\} \quad (\text{Eq. B.10})$$

$$= \sum_{k=1}^N b_k \cdot a_k \cdot \exp\{j\omega(T_{kS} - T_{kF})\} \quad (\text{Eq. B.11})$$

$$= \sum_{k=1}^N w_k \exp\{j\theta_k\} \quad , \quad (\text{Eq. B.12})$$

where

b_k = amplitude response of the receiving physical array in the direction of the scatterer S.

a_k = amplitude shading factor that can be used to suppress the side-lobes of the synthesized beam, if required.

ωT_{kF} = phase shift of the echo relative to first transmission, required to focus the synthesized beam to position F.

ωT_{kS} = actual phase shift of the echo from the scatterer position S.

$$\omega_k = b_k \cdot a_k \quad (\text{Eq. B.13})$$

$$\omega = 2\pi f \quad (\text{Eq. B.14})$$

where f is the frequency of the transmitted signal.

The phase shift θ_k of Eq. B.12 is calculated based on the geometry of Fig. B1 and the timing sequence of Fig. B2.

From the relations (Fig. B1)

$$(\nu \Delta t_{kF})^2 + R_{kS}^2 - 2\nu \Delta t_{kF} R_{kS} \cdot \cos(\pi/2 - \alpha_{kF}) = R_{kF}^2 \quad (\text{Eq. B.15})$$

$$\Delta t_{kF} = \frac{R_{kF}^I + R_{kF}^{II}}{c} \quad (\text{Eq. B.16})$$

we obtain

$$\frac{R_{kF}^{II}}{R_{kF}^I} = \frac{\frac{\nu}{c} \left(\frac{\nu}{c} - \sin \alpha_{kF} \right) + \left\{ \left[\frac{\nu}{c} \left(\frac{\nu}{c} - \sin \alpha_{kF} \right) \right]^2 + \left[1 - \left(\frac{\nu}{c} \right)^2 \right] \left[\frac{\nu}{c} \left(\frac{\nu}{c} - 2 \sin \alpha_{kF} \right) + 1 \right] \right\}^{\frac{1}{2}}}{1 - \left(\frac{\nu}{c} \right)^2} \quad (\text{Eq. B.17})$$

From Eqs. B.15, B.16 and B.17 we derive:

$$\Delta t_{kF} = \frac{R_{kF}^I}{c \left[1 - \left(\frac{\nu}{c} \right)^2 \right]} \cdot \left\{ 1 + \frac{\nu}{c} \left(\frac{\nu}{c} - \sin \alpha_{kF} \right) + \left[\frac{\nu}{c} \left(\frac{\nu}{c} - \sin \alpha_{kF} \right) \right]^2 + \left[1 - \left(\frac{\nu}{c} \right)^2 \right] \cdot \left[\frac{\nu}{c} \left(\frac{\nu}{c} - 2 \sin \alpha_{kF} \right) + 1 \right]^{\frac{1}{2}} \cdot \left[1 - \left(\frac{\nu}{c} \right)^2 \right]^{-1} \right\} \quad (\text{Eq. B.18})$$

From Fig. B1 we also derive:

$$R_{kF}^I{}^2 + 2\nu T_{kF} R_{kF}^I \sin \alpha_{kF} + (\nu T_{kF})^2 = R_{oF}^2 \quad (\text{Eq. B.19})$$

$$R_{kF}^I = -\nu T_{kF} \sin \alpha_{kF} + \{ R_{oF}^2 - (\nu T_{kF} \cos \alpha_{kF})^2 \}^{\frac{1}{2}} \quad (\text{Eq. B.20})$$

The angle α_{kF} is calculated from (see Fig. B1):

$$R_o \tan \beta_m = R_o \tan \beta_F + R_o \tan \alpha_{kF} + vT_{kF} \quad (\text{Eq. B.21})$$

$$R_o \tan \beta_m = v \cdot T/2, \quad (\text{Eq. B.22})$$

where T is the total integration time.

We obtain for α_{kF} :

$$\alpha_{kF} = \arctan \left\{ \left(1 - \frac{2T_{kF}}{T}\right) \tan \beta_m - \tan \beta_F \right\}, \quad (\text{Eq. B.23})$$

where T_{kF} is calculated by Eq. B.7.

For Δt_{kS} we obtain similarly:

$$\Delta t_{kS} = \frac{R'_{kS}}{c \left[1 - \left(\frac{v}{c}\right)^2\right]} \cdot \left[1 + \frac{v}{c} \left(\frac{v}{c} - \sin \alpha_{kS}\right) + \left\{ \left[\frac{v}{c} \left(\frac{v}{c} - \sin \alpha_{kS}\right)\right]^2 + \left[1 - \left(\frac{v}{c}\right)^2\right] \cdot \left[\frac{v}{c} \left(\frac{v}{c} - 2 \sin \alpha_{kS}\right)\right] + 1 \right\}^{\frac{1}{2}} \cdot \left[1 - \left(\frac{v}{c}\right)^2\right]^{-1}\right] \quad (\text{Eq. B.24})$$

with

$$R'_{kS} = -vT_{kS} \sin \alpha_{kS} + \{R_o^2 - (vT_{kF} \cos \alpha_{kS})^2\}^{\frac{1}{2}} \quad (\text{Eq. B.25})$$

and the angle α_{kS} is given by:

$$\alpha_{kS} = \arctan \left\{ \left(1 - \frac{2T_{kF}}{T}\right) \tan \beta_m - \tan \beta_S \right\} \quad (\text{Eq. B.26})$$

The phase shift θ_k is calculated from Eq. B14 using Eqs. B.9, B.18, and B.24.

Equation B.20 can also be written for the generic time $t = t_k$ in the form:

$$R'_k = -vt_k \sin \alpha_k + \left[R_o^2 \left(1 - \frac{(vt_k \cos \alpha_k)^2}{R_o^2}\right) \right]^{\frac{1}{2}} \quad (\text{Eq. B.27})$$

In the approximation of far-field (i.e. $vt_k/R_o \ll 1$) we have:

$$R'_k \approx -vt_k \sin \alpha_k + R_o \left[1 - \frac{(vt_k \cos \alpha_k)^2}{2R_o^2}\right] \quad (\text{Eq. B.28})$$

or

$$R'_k \approx -vt_k \sin \alpha_k + R_0 - \frac{(vt_k \cos^2 \alpha_k)}{2R_0} \cong R_0 - vt_k \sin \alpha_k \quad (\text{Eq. B.29})$$

From Eq. B.17, in the approximation of $v/c \ll 1$ we can also derive:

$$R''_k \approx R'_k \left[\frac{v}{c} \left(\frac{v}{c} - \sin \alpha_k \right) + \left(1 - \frac{2v}{c} \sin \alpha_k \right)^{\frac{1}{2}} \right] \quad (\text{Eq. B.30})$$

or

$$R''_k \approx R'_k \left(1 - \frac{2v}{c} \sin \alpha_k \right) \quad (\text{Eq. B.31})$$

the times Δt_{kS} and Δt_{kF} are given from the above assumptions by:

$$\Delta t_{kF} \approx \left[R'_{kF} + R'_{kF} \left(1 - \frac{2v}{c} \sin \alpha_{kF} \right) \right] \frac{1}{c} \quad (\text{Eq. B.32})$$

$$\Delta t_{kF} \approx \frac{2R'_{kF}}{c} \left(1 - \frac{2v}{c} \sin \alpha_{kF} \right) \quad (\text{Eq. B.33})$$

$$\Delta t_{kF} \approx \frac{2}{c} \left[\left(R_0 - vT_{kF} \sin \alpha_{kF} \right) \left(1 - \frac{v}{c} \sin \alpha_{kF} \right) \right] \quad (\text{Eq. B.34})$$

similarly for Δt_{kS} :

$$\Delta t_{kS} \approx \frac{2R'_{kS}}{c} \left(1 - \frac{v}{c} \sin \alpha_{kS} \right) \quad (\text{Eq. B.35})$$

$$\Delta t_{kS} \approx \frac{2}{c} \left[\left(R_0 - vT_{kS} \sin \alpha_{kS} \right) \left(1 - \frac{v}{c} \sin \alpha_{kS} \right) \right] \quad (\text{Eq. B.36})$$

The difference $\Delta t_{kF} - \Delta t_{kS}$ is computed from Eqs. B.34 and B.36:

$$\left[\frac{2v}{c} T_{kF} + \frac{R_0}{c} - \frac{2v^2 T_{kF}}{c^2} (\sin \alpha_{kF} + \sin \alpha_{kS}) \right] (\sin \alpha_{kS} - \sin \alpha_{kF}) \quad (\text{Eq. B.37})$$

The synthesized beam voltage is given by the sum:

$$V = \sum_{k=1}^N w_k \exp \left[-\frac{2j\omega}{c} (\Delta t_{kF} - \Delta t_{kS}) \right] \quad (\text{Eq. B.38})$$

If we assume, in the far-field, $\alpha_{kS} \approx \alpha_{kF}$:

$$(\sin \alpha_{kS} + \sin \alpha_{kF}) \cdot (\sin \alpha_{kS} - \sin \alpha_{kF}) \approx 2 \sin \alpha_{kF} (\sin \alpha_{kS} - \sin \alpha_{kF}) \quad (\text{Eq. B.39})$$

Therefore, from Eqs. B.37 and B.38 we obtain:

$$V \approx \sum_{k=1}^N w_k \exp \left[-\frac{2j\omega v}{c} T_{kF} \left(1 + \frac{4v}{c} \sin \alpha_{kF} \right) \cdot (\sin \alpha_{kS} - \sin \alpha_{kF}) \right] \quad (\text{Eq. B.40})$$

Under the assumption of $\frac{v}{c} \sin \alpha_{kF} \ll 1$

$$V \approx \sum_{k=1}^N w_k \exp \left[-\frac{2j\omega v}{c} T_{kF} \cdot (\sin \alpha_{kS} - \sin \alpha_{kF}) \right] \quad (\text{Eq. B.41})$$

where T_{kF} is given by Eq. B.7.

In the far-field, the difference between the sampling intervals becomes very small. Therefore, if we assume that:

$$T_{kF} = k\Delta\tau \quad (\text{Eq. B.42})$$

and in the small angle approximation:

$$\alpha_{kS} \approx \frac{\beta_m}{2} - \beta_m \cdot \frac{k}{N} - \beta_S \quad (\text{Eq. B.43})$$

$$\alpha_{kF} \approx \frac{\beta_m}{2} - \beta_m \cdot \frac{k}{N} - \beta_F \quad (\text{Eq. B.44})$$

we obtain for the beam voltage:

$$V \approx \sum_{k=1}^N \exp \left[\frac{2j\omega v}{c} k\Delta\tau \cdot (\sin \alpha_{kS} - \sin \alpha_{kF}) \right] \quad (\text{Eq. B.45})$$

The synthesized beam pattern is then:

$$V \cdot V^* = \left[\frac{\sin\left(\frac{Nwv\Delta\tau}{c} \sin\psi\right)}{\sin\left(\frac{wv\Delta\tau}{c} \sin\psi\right)} \right]^2 \equiv \left[\frac{\sin\left(2N \frac{\pi d}{c} \sin\psi\right)}{\sin\left(\frac{\pi d}{c} \sin\psi\right)} \right]^2 \quad (\text{Eq. B.46})$$

which is the standard form for a linear array in far-field conditions and composed by N hydrophones uniformly spaced by d .

Equation B.46 represents the beam pattern formed with $2N$ samples. That is, the effective synthesized aperture is $2Nd$. Consequently the active synthesized beam pattern has a 3 dB beamwidth, which is half of that for a normal passive array of the same length. Also, as discussed in par. 2.4, the active synthetic aperture array differs from the normal active array, which would have a beamwidth forty percent greater for the same length.

B2 Beamforming in the presence of random amplitude and phase errors

The synthetic beam former makes the sum of N echoes:

$$V = \sum_{k=1}^N \tilde{s}_k \quad (\text{Eq. B.47})$$

The k -th component is given by:

$$\tilde{s}_k = \tilde{w}_k \exp(j\tilde{\theta}_k) \quad (\text{Eq. B.48})$$

with:

$$\tilde{w}_k = w_k + \eta_k \quad (\text{Eq. B.49})$$

where η_k is a random amplitude fluctuation term.

And with:

$$\tilde{\theta}_k = \theta_k + \varepsilon_k \quad (\text{Eq. B.50})$$

where ε_k is a random phase jitter.

From Eqs. B.47, B.48, B.49 and B.50 we have:

$$V = \sum_{k=1}^N (w_k + \eta_k) \exp\{j(\theta_k + \varepsilon_k)\} \quad (\text{Eq. B.51})$$

and

$$p_k = (w_k + \eta_k) \sin(\theta_k + \varepsilon_k) \quad (\text{Eq. B.59})$$

For the analysis of beamforming we assume that the two random variables ε_k and η_k are:

- a. Mutually independent
- b. Correlated in time

Under the first assumption, from Eqs. B.58 and B.59 we have:

$$E\{r_k^2\} = E\{(w_k + \eta_k)^2\} \cdot E\{\cos^2(\theta_k + \varepsilon_k)\} \quad (\text{Eq. B.60})$$

$$E\{p_k^2\} = E\{(w_k + \eta_k)^2\} \cdot E\{\sin^2(\theta_k + \varepsilon_k)\} \quad (\text{Eq. B.61})$$

and

$$E\{r_k \cdot r_{k+i}\} = E\{(w_k + \eta_k) \cos(\theta_k + \varepsilon_k) \cdot (w_{k+i} + \eta_{k+i}) \cos(\theta_{k+i} + \varepsilon_{k+i})\} \quad (\text{Eq. B.62})$$

$$E\{p_k \cdot p_{k+i}\} = E\{(w_k + \eta_k) \sin(\theta_k + \varepsilon_k) \cdot (w_{k+i} + \eta_{k+i}) \sin(\theta_{k+i} + \varepsilon_{k+i})\} \quad (\text{Eq. B.63})$$

or

$$E\{r_k \cdot r_{k+i}\} = E\{(w_k + \eta_k) \cdot (w_{k+i} + \eta_{k+i})\} \cdot E\{\cos(\theta_k + \varepsilon_k) \cdot \cos(\theta_{k+i} + \varepsilon_{k+i})\} \quad (\text{Eq. B.64})$$

$$E\{p_k \cdot p_{k+i}\} = E\{(w_k + \eta_k) \cdot (w_{k+i} + \eta_{k+i})\} \cdot E\{\sin(\theta_k + \varepsilon_k) \cdot \sin(\theta_{k+i} + \varepsilon_{k+i})\} \quad (\text{Eq. B.65})$$

The expected beam power output is therefore given by:

$$E\{V \cdot V^*\} = \sum_{k=1}^N q_k^2 + 2 \sum_{i=1}^{N-1} \sum_{k=1}^{N-i} q_k q_{k+i} \cdot [E\{\cos(\theta_k + \varepsilon_k) \cdot \cos(\theta_{k+i} + \varepsilon_{k+i})\} + E\{\sin(\theta_k + \varepsilon_k) \cdot \sin(\theta_{k+i} + \varepsilon_{k+i})\}] \quad (\text{Eq. B.66})$$

where

$$q_k^2 = E\{(w_k + \eta_k)^2\}; \quad q_k q_{k+i} = E\{(w_k + \eta_k) \cdot (w_{k+i} + \eta_{k+i})\} \quad (\text{Eq. B.67})$$

Considering the trigonometric relation:

$$\begin{aligned}
 & \cos(\theta_k + \varepsilon_k) \cdot \cos(\theta_{k+i} + \varepsilon_{k+i}) + \sin(\theta_k + \varepsilon_k) \cdot \sin(\theta_{k+i} + \varepsilon_{k+i}) \\
 &= \cos(\theta_k + \varepsilon_k - \theta_{k+i} - \varepsilon_{k+i}) \cos\{(\theta_k - \theta_{k+i}) + (\varepsilon_k - \varepsilon_{k+i})\} \\
 &= \cos(\theta_k - \theta_{k+i}) \cdot \cos(\varepsilon_k - \varepsilon_{k+i}) - \sin(\theta_k - \theta_{k+i}) \sin(\varepsilon_k - \varepsilon_{k+i})
 \end{aligned} \tag{Eq. B.68}$$

Equation B.66 can be written:

$$\begin{aligned}
 E\{V \cdot V^*\} &= \sum_{k=1}^N q_k^2 + 2 \sum_{i=1}^{N-1} \sum_{k=1}^{N-i} q_k q_{k+i} \cdot [\cos(\theta_k - \theta_{k+i}) \cdot E\{\cos(\varepsilon_k - \varepsilon_{k+i})\} - \\
 & \quad \sin(\theta_k - \theta_{k+i}) \cdot E\{\sin(\varepsilon_k - \varepsilon_{k+i})\}]
 \end{aligned} \tag{Eq. B.69}$$

In the approximation of small errors:

$$E\{\sin(\varepsilon_k - \varepsilon_{k+i})\} \approx E\{\varepsilon_k - \varepsilon_{k+i}\} = 0 \tag{Eq. B.70}$$

$$E\{\cos(\varepsilon_k - \varepsilon_{k+i})\} \approx E\left\{1 - \frac{(\varepsilon_k - \varepsilon_{k+i})^2}{2}\right\} = 1 - \frac{1}{2} [E\{\varepsilon_k^2\} + E\{\varepsilon_{k+i}^2\} - 2E\{\varepsilon_k \cdot \varepsilon_{k+i}\}] \tag{Eq. B.71}$$

The expected value of the beam power output is:

$$\begin{aligned}
 E\{V \cdot V^*\} &= \sum_{k=1}^N q_k^2 + 2 \sum_{i=1}^{N-1} \sum_{k=1}^{N-i} q_k q_{k+i} \cdot \left\{ \cos(\theta_k - \theta_{k+i}) \cdot \right. \\
 & \quad \left. \left[1 - \frac{1}{2} E\{\varepsilon_k^2\} - \frac{1}{2} E\{\varepsilon_{k+i}^2\} + E\{\varepsilon_k \cdot \varepsilon_{k+i}\} \right] \right\}
 \end{aligned} \tag{Eq. B.72}$$

From Eqs. B.67, B.68, B.69, B.70, B.71 and B.72 we derive:

$$\begin{aligned}
 E\{V \cdot V^*\} &= \sum_{k=1}^N E\{w_k^2\} + E\{\eta_k^2\} + 2 \sum_{i=1}^{N-1} \sum_{k=1}^{N-i} [E\{w_k \cdot w_{k+i}\} + E\{\eta_k \cdot \eta_{k+i}\}] \cdot \\
 & \quad \left[1 - \frac{1}{2} E\{\varepsilon_k^2\} - \frac{1}{2} E\{\varepsilon_{k+i}^2\} + E\{\varepsilon_k \cdot \varepsilon_{k+i}\} \right] \cos(\theta_k - \theta_{k+i})
 \end{aligned} \tag{Eq. B.73}$$

It is assumed that the random phase jitter ε_k and the random fluctuation in the amplitude η_k are described by a stationary Markov process of the first order. Thus the conditions on ε_k and η_k are:

Zero-mean

$$E\{\varepsilon_k\} = E\{\eta_k\} = 0 \quad (\text{Eq. B.74})$$

with variances:

$$E\{\varepsilon_k^2\} = \sigma_{\varepsilon_k}^2, \quad E\{\eta_k^2\} = \sigma_{\eta_k}^2 \quad (\text{Eq. B.75})$$

and correlation given by:

$$E\{\varepsilon_k \cdot \varepsilon_{k+i}\} = \sigma_{\varepsilon_k}^2 \cdot \exp[-|t_k - t_{k+i}|/\tau_1] \quad (\text{Eq. B.76})$$

$$E\{\eta_k \cdot \eta_{k+i}\} = \sigma_{\eta_k}^2 \cdot \exp[-|t_k - t_{k+i}|/\tau_2] \quad (\text{Eq. B.77})$$

with τ_1 and τ_2 time constant of the fluctuations of phase and amplitude respectively.

Stationarity of phase and amplitude fluctuations implies that:

$$E\{\varepsilon_k^2\} = E\{\varepsilon_{k+i}^2\} \quad (\text{Eq. B.78})$$

and

$$E\{\eta_k^2\} = E\{\eta_{k+i}^2\} \quad (\text{Eq. B.79})$$

In the condition of a stationary signal, i. e.

$$E\{w_k^2\} = E\{w_{k+i}^2\}, \quad (\text{Eq. B.80})$$

by combining Eqs. B.74 to B.80 we obtain for the expected beam power output the expression:

$$E\{V \cdot V^*\} = \sum_{k=1}^N (E\{w_k^2\} + \sigma_{\eta_k}^2) + 2 \sum_{i=1}^{N-1} \sum_{k=1}^{N-i} \{E\{w_k^2\} + \sigma_{\eta_k}^2 \exp\{-|t_k - t_{k+i}|/\tau_1\}\} \cdot [1 - \sigma_{\varepsilon_k}^2 (1 - \exp\{-|t_k - t_{k+i}|/\tau_2\})] \cdot \cos(\theta_k - \theta_{k+i}) \quad (\text{Eq. B.81})$$

where θ_k is the phase calculated from the geometry of Fig. B1 in the absence of any errors (see Eq. B.12).

B3 Analysis of Placement Errors

Based on the geometry of Fig. B3 we calculate the placement error given by the difference:

$$\Delta_{kT} = (r'_{kT} + r''_{kT}) - (R'_{kT} + R''_{kT}) \quad (\text{Eq. B.82})$$

The second quantity of the right side of Eq. B.82 is defined by the geometry of the ideal case of straight-line course (see Fig. B1).

The first quantity is computed from (see Fig. B3):

$$r'_{kT} = \delta_k'^2 + R_{kT}'^2 - 2\delta_k' R_{kT}' \cos[\alpha_{kS}' + \frac{\pi}{2} + \arctan \frac{y_k^*}{x_k^*}] \quad (\text{Eq. B.83})$$

$$r''_{kT} = \delta_k''^2 + R_{kT}''^2 - 2\delta_k'' R_{kT}'' \cos[\alpha_{kS}'' + \frac{\pi}{2} + \arctan \frac{y_k^{**}}{x_k^{**}}] \quad (\text{Eq. B.84})$$

where

α_{kS}' and α_{kS}'' are the aspect angles of the target as defined in the straight-line path geometry.

$$\delta_k' = [y_k^{*2} + (x_k - x_k^*)^2]^{\frac{1}{2}} \quad (\text{Eq. B.85})$$

$$\delta_k'' = [y_k^{**2} + (x_k - x_k^{**})^2]^{\frac{1}{2}} \quad (\text{Eq. B.86})$$

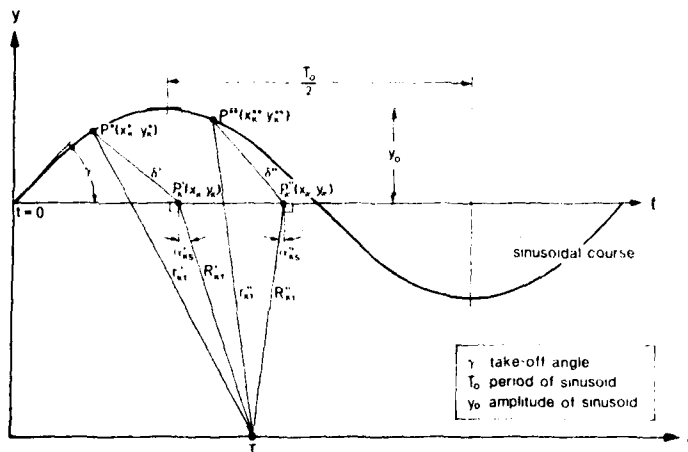


FIG. B3 GEOMETRY OF PLACEMENT ERRORS (Active operation)

The coordinates of the points $P^*(x_k^*, y_k^*)$, $P^{**}(x_k^{**}, y_k^{**})$ are computed by the integrals:

$$x_k^* = \int_{t_0}^{t_k} U_{xt} dt, \quad y_k^* = \int_{t_0}^{t_k} U_{yt} dt \quad (\text{Eq. B.87})$$

$$x_k^{**} = \int_{t_0}^{t_{k1}} U_{xt} dt, \quad y_k^{**} = \int_{t_0}^{t_{k1}} U_{yt} dt \quad (\text{Eq. B.88})$$

B.3.1 Calculation of U_{xt}

From the geometrical relation:

$$U_{xt}^2 + U_{yt}^2 = U^2 \quad (\text{Eq. B.89})$$

Assuming for the y-component of the velocity:

$$U_{yt} = U \sin \gamma \cdot \cos \left(\frac{2\pi t}{T_0} \right) \quad (\text{Eq. B.90})$$

combining Eqs. B.89 and B.90 and using the fact that $\sin^2 \gamma \cdot \cos^2 \frac{2\pi t}{T_0}$ is always small, we obtain:

$$U_{xt} = U \left\{ 1 - \frac{\sin^2 \gamma}{2} \cdot \cos^2 \frac{2\pi t}{T_0} \right\} \quad (\text{Eq. B.91})$$

B.3.2 Calculation of x_k^*, y_k^*

From Eqs. B.87 and B.90 we calculate the abscissa of P^* :

$$x_k^* = U \left\{ t_k \left(1 - \frac{\sin^2 \gamma}{4} \right) - \frac{T_0}{16\pi} \sin^2 \gamma \left(\sin \frac{4\pi t_k}{T_0} \cdot \sin \frac{4\pi t_0}{T_0} \right) + \frac{\sin^2 \gamma_0}{4} \cdot t_0 \right\} \quad (\text{Eq. B.92})$$

From Eqs. B.87 and B.90 we calculate the ordinate of P^* :

$$y_k^* = \frac{UT_0}{2\pi} \sin \gamma \cdot \left[\sin \frac{2\pi t_k}{T_0} - \sin \frac{2\pi t_0}{T_0} \right] \quad (\text{Eq. B.93})$$

B.3.3 Calculation of x_k^{**}, y_k^{**}

From the integrals of Eq. B.88 and Eqs. B.90 and B.91 we compute the coordinates of p^{**} :

$$x_k^{**} = U \left\{ t_{k1} \left(1 - \frac{\sin^2 \gamma}{4} \right) - \frac{T_0}{16\pi} \sin^2 \gamma \left(\sin \frac{4\pi t_{k1}}{T_0} \cdot \sin \frac{4\pi t_0}{T_0} \right) + \frac{\sin^2 \gamma_0}{4} \cdot t_0 \right\} \quad (\text{Eq. B.94})$$

$$y_k^{**} = \frac{UT_0}{2\pi} \sin \gamma \cdot \left[\sin \frac{2\pi t_{k1}}{T_0} - \sin \frac{2\pi t_0}{T_0} \right] \quad (\text{Eq. B.95})$$

The time t_{k1} corresponding to the position p^{**} is calculated in the computer model by the expression:

$$t_{k1} = t_k + 2 \frac{r'_{kT}}{c} \quad (\text{Eq. B.96})$$

which minimizes the difference between the "true" time TS and the measured TSE. For TS we assume the arithmetic mean:

$$TS = \left(2 \frac{r'_{kT}}{c} + TSE \right) \cdot \frac{1}{2} \quad (\text{Eq. B.97})$$

SACI.ANTCEN SR-91

KEYWORDS

ACTIVE SYNTHETIC APERTURE PROCESSING
AMPLITUDE ERROR
BEAMFORMING
DETERMINISTIC PLACEMENT ERROR
PASSIVE SYNTHETIC APERTURE PROCESSING
RANDOM PHASE ERROR
SIGNAL COHERENCE
SYNTHESIZED BEAMPATTERN
SYNTHETIC APERTURE SONAR

INITIAL DISTRIBUTION

	Copies		Copies
<u>MINISTRIES OF DEFENCE</u>		<u>SCNR FOR SACLANTCEN</u>	
JSPHQ Belgium	2	SCNR Belgium	1
DND Canada	10	SCNR Canada	1
CHOD Denmark	8	SCNR Denmark	1
MOD France	8	SCNR Germany	1
MOD Germany	15	SCNR Greece	1
MOD Greece	11	SCNR Italy	1
MOD Italy	10	SCNR Netherlands	1
MOD Netherlands	12	SCNR Norway	1
CHOD Norway	10	SCNR Portugal	1
MOD Portugal	2	SCNR Turkey	1
MOD Spain	2	SCNR U.K.	1
MOD Turkey	5	SCNR U.S.	2
MOD U.K.	20	SECGEN Rep. SCNR	1
SECDEF U.S.	65	NAMILCOM Rep. SCNR	1
<u>NATO AUTHORITIES</u>		<u>NATIONAL LIAISON OFFICERS</u>	
Defence Planning Committee	3	NLO Canada	1
NAMILCOM	2	NLO Denmark	1
SACLANT	10	NLO Germany	1
SACLANTREPEUR	1	NLO Italy	1
CINWESTLANT/COMOCEANLANT	1	NLO U.K.	1
COMSTRIKFLTANT	1	NLO U.S.	1
COMIBERLANT	1		
CINCEASTLANT	1	<u>NLR TO SACLANT</u>	
COMSUBACLANT	1	NLR Belgium	1
COMMAIREASTLANT	1	NLR Canada	1
SACEUR	2	NLR Denmark	1
CINCNORTH	1	NLR Germany	1
CINCSOUTH	1	NLR Greece	1
COMNAVSOUTH	1	NLR Italy	1
COMSTRIKFORSOUTH	1	NLR Netherlands	1
COMEDCENT	1	NLR Norway	1
COMMAIRMED	1	NLR Portugal	1
CINCHAN	3	NLR Turkey	1
		NLR UK	1
		NLR US	1
		Total initial distribution	286
		SACLANTCEN Library	10
		Stock	24
		Total number of copies	280